Soils and Rocks

www.soilsandrocks.com

An International Journal of Geotechnical and Geoenvironmental Engineering

ISSN 1980-9743
ISSN-e 2675-5475

Soil-atmosphere interaction in geotechnics: some aspects concerning gravitational soil mass movements and biogas production and emissions in tropical environment

Tácio Mauro Pereira de Campos[1#], Mariana Ferreira Benessiuti Motta[2], Nicolas Rodrigues Moura[1], Elisangela do Prado Oliveira[3], Álvaro de Freitas Viana[1], José Camapum de Carvalho[4], José Fernando Thomé Jucá[5], Sandro Lemos Machado[6]

Article

Keywords
Soil-atmosphere interaction
Soil cracking
Erosion
Slope stability analysis
Thunderstorms
Sanitary landfills

Abstract

Soil-atmosphere interactions comprise a multidisciplinary and transdisciplinary subject of interest to numerous applied and research knowledge areas. In this work, aspects related to geotechnical, geoenvironmental and geological engineering, not usually considered in applied civil or environmental engineering projects, are put forward, exemplifying the role that micro-climatic conditions may have in the development of gravitational soil mass movements such as erosion processes and natural slope stability comprising unsaturated tropical soils. Based on literature data, proposals are put forward to consider cracks that develop under dry climatic conditions in engineering projects. Additionally, laboratory testing results indicate that the shear strength of soils may decrease due to climatic dry-wetting cycles, potentially compromising the accuracy of slope stability analysis results. In addition, the need to evaluate initial soil-water profile conditions in flow analysis is presented and discussed under various scenarios, and the effects of further atmospheric events, such as lightning, are also presented and discussed. Furthermore, based on data collected from diverse Brazilian sanitary landfills designed to operate primarily on municipal solid waste, relationships between soil-atmospheric variables and biogas generation and emission are investigated. Finally, based on the results generated in a physical model, a type of final municipal landfill cover is presented and discussed, whose design strongly depends on atmospheric data.

1. Introduction

Soil-atmosphere interactions encompass a multidisciplinary and transdisciplinary subject of interest to numerous areas of knowledge, including geosciences, soil science, agronomy, geography, hydrology, ecology, climatology, civil engineering, geological engineering, and environmental engineering. Atmospheric conditions affect the climate and meteorological scenarios prevailing in a specific region or site. This contributes, along with geological and geomorphological conditions, to the formation of soil profiles through variable weathering processes that occur over geological time scales (e.g., van Breemen & Buurman, 2002; Chai et al., 2015; Conciani et al., 2023). In this context, soil-atmosphere interactions have long been of interest. However, physical-chemical-mineralogical and, consequently, hydro-mechanical properties of soil profiles may vary along human time scales due to changes in the physical environment imposed by anthropic actions (e.g., carbon dioxide emissions, changes in hydrogeological conditions, acidic rain production and natural drainage path changes), and variations of climatic conditions (e.g., extreme temperatures, rainstorms intensity raise and rainfall

[#]Corresponding author. E-mail address: tacio@puc-rio.br
[1]Pontifícia Universidade Católica do Rio de Janeiro, Departamento de Engenharia Civil e Ambiental, Rio de Janeiro, RJ, Brasil.
[2]Universidade Estadual Paulista, Departamento de Engenharia Civil, Guaratinguetá, SP, Brasil.
[3]Universidade Federal do Paraná, Centro de Estudos do Mar, Pontal do Paraná, PR, Brasil.
[4]Universidade de Brasília, Departamento de Engenharia Civil e Ambiental, Brasília, DF, Brasil.
[5]Universidade Federal de Pernambuco, Departamento de Engenharia Civil e Ambiental, Recife, PE, Brasil.
[6]Universidade Federal da Bahia, Escola Politécnica, Salvador, BA, Brasil.

Submitted on January 31, 2025; Final Acceptance on April 12, 2025; Discussion open until November 30, 2025.

Editor: Renato P. Cunha

https://doi.org/10.28927/SR.2025.001825

distribution change) at a given region or site. Thus, soil-atmosphere interactions have become a significant research topic today, particularly in the context of global reporting on extreme climatic variations (e.g., Marengo et al., 2021; Brasil, 2021; IPCC, 2023; Dunn et al., 2024).

Bearing in mind the above and considering the geotechnical and geoenvironmental aspects, soil-atmosphere interactions have been studied. They are being increasingly investigated by various authors with differing research interests, as exemplified in Table 1.

Table 1. Examples of soil-atmosphere interactions aspects being investigated within the geotechnical and geoenvironmental areas.

Subject		References
(a) Stability aspects	unsaturated, natural or cut slopes	Rianna et al. (2016); Tsiampousi et al. (2016); de Campos et al. (2018); Bordoni et al. (2021); Chen et al. (2024)
	rock slopes	Vargas Junior et al. (2013); Collins & Stock (2016); Soukatchoff & Barbier (2023); Stoffel et al. (2024)
	earthen structures	Ghosh et al. (2024)
	retaining walls / reinforced slopes	Speranza et al. (2022); Melo et al. (2023); Tian et al. (2023)
	sanitary landfills	Jucá et al. (2021)
	mine tailings dams / piles	Kossoff et al. (2014); Maknoon & Aubertin (2021); Clarkson & Williams (2021); Zhang et al. (2024)
(b) Erosion processes development in the natural ground and earthen structures		Almagro et al. (2017); Joris et al. (2022); Mandal & Roy (2024); de Carvalho et al. (2025)
(c) Greenhouse or toxic gas emissions from landfills and agricultural areas		Langenbach et al. (2017); Damasceno et al. (2019); Gama et al. (2019); IEA (2023)
(d) Contaminant transport underground		Ahmadi et al. (2022)
(e) Storage and retention of Carbon in the soil		Kramer & Chadwick (2018); Heckman et al. (2023)

From the viewpoint of geotechnics, regardless of the biological or biochemical processes that may be relevant to a given site, soil-atmosphere processes, essentially comprising unsaturated soil wetting and drying conditions, are summarized in Figure 1. This figure, modified from Borma et al. (2023), illustrates a generic soil profile distribution in terms of saturation degree and water table level. In the saturated soil zone, fluxes occur between the water table and the unsaturated soil zone, while in the latter zone, fluxes occur between the saturated zone and the atmosphere. In any case, water and heat flows, related respectively to hydric and energy balances, act simultaneously, implying complex interaction processes between water infiltration into and evaporation out of the soil profile, not always easy to model (e.g., Hillel, 1998; Borma et al., 2013; Stocker et al., 2013; Cui, 2022).

1.1 Active zone

The depth up to which atmospheric changes affect conditions in the near soil surface (active zone in Figure 1) depends on factors such as land use, soil cover, soil profile, depth of the water level and water balance. As shown in Figure 2 (Khalili et al., 2022), such depth may vary from some 1 to 6 m depth, according to the climate of the region or site, expressed by the Thornthwaite Moisture Index - TMI (Thornthwaite, 1948; Fityus et al., 1998; Olaiz et al., 2017; Karim et al., 2024). Considering water balance, Figure 2 suggests that the thickness of the active zone may be more relevant in regions of dryer climates. However, TMI alone may not always represent conditions at specific sites (e.g., Thornthwaite & Mather, 1955, 1957; Andrade, 2019). Indeed, a better definition of the depth of the active zone requires, typically, monitoring of variables such as temperature, soil suction, and/or moisture content variations over time. However, it must be considered that such thickness may vary according to the variable under consideration and where the instrumentation was installed in the soil profile. An example of that is given in Figure 3, which shows the results of temperature and volumetric water content measurements taken along depth in a plateau and at the slope surface of a given site (An et al., 2017). In this figure, measurements based on temperature indicate active zone depths above 4 m in the plateau area and below 4 m in the slope face. Measurements based on volumetric water content indicate an active zone above 2 m depth due to water infiltration in the plane area (changes below 4 m in Figure 3c probably reflect interferences of the water table) and below 3 m depth in the open slope area.

Summarizing, together with boundary conditions regarding human interventions associated with geological and geomorphological features, and consequently, bio-physical-chemical and hydro-mechanical soil property variations, evaluation of climatic characteristics is mandatory in assessing susceptibilities to failure and excessive deformation

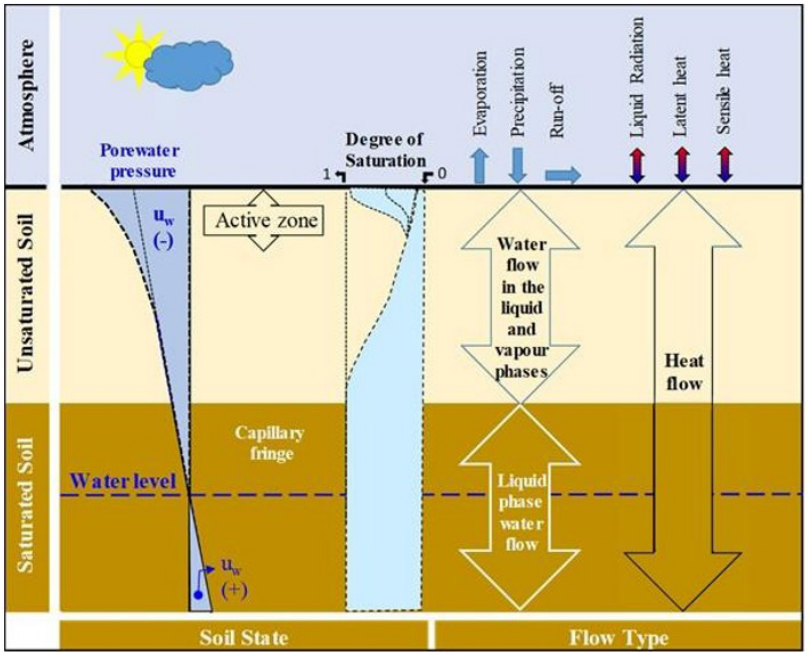

Figure 1. Fluxes at the soil-atmosphere interface and the saturated-unsaturated soil zone interfaces. Not at scale. Adapted from Borma et al. (2023).

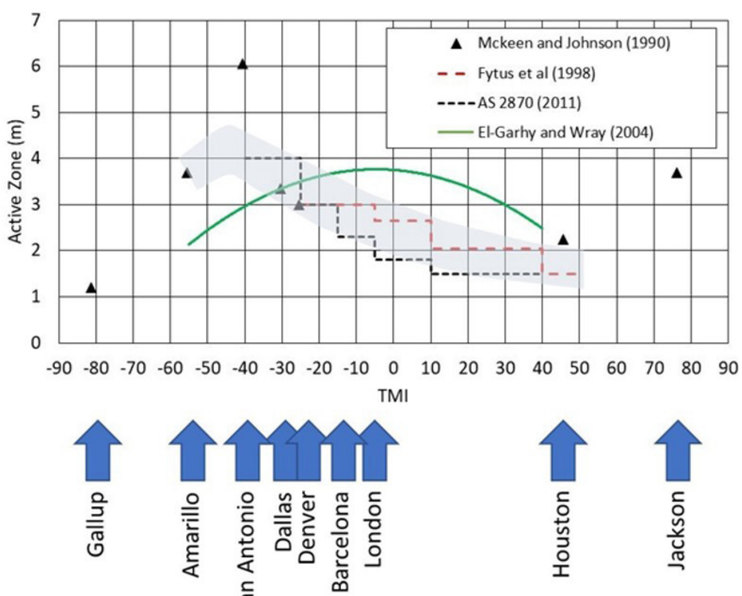

Climate Category*	TMI
Prehumid - A	≥100
Humid - B4	80 to 100
Humid - B3	60 to 80
Humid - B2	40 to 60
Humid - B1	20 to 40
Moist Humid - C2	0 to 20
Dry subhumid - C1	-20 to 0
Semiarid - D	-40 to -20
Arid - E	-60 to -40

*Thornthwaite (1948)

Figure 2. Association between active zone and TMI. Adapted from Khalili et al. (2022).

processes, as well as evolved mechanisms in geotechnical engineering as a whole. In this sense, knowledge of regional and local weather regimes or hydric balance is crucial.

In the present work, this wide and complex subject is dealt with by considering some particular aspects related to soil-atmosphere issues comprising:

i) simulation of hydric balance and cracks formation under soil drying, relevant to analyses of effects of soil-atmosphere interaction in any area of interest,
ii) development of soil-erosion processes and potential microclimatic effects,
iii) slope stability analysis with emphasis on evaluation of initial suction profiles in unsaturated soil slopes and effects of drying in shear strength parameters,
iv) further atmospheric potential effects on gravitational mass movements,
v) soil-atmosphere interactions on biogas production and emissions from sanitary landfills.

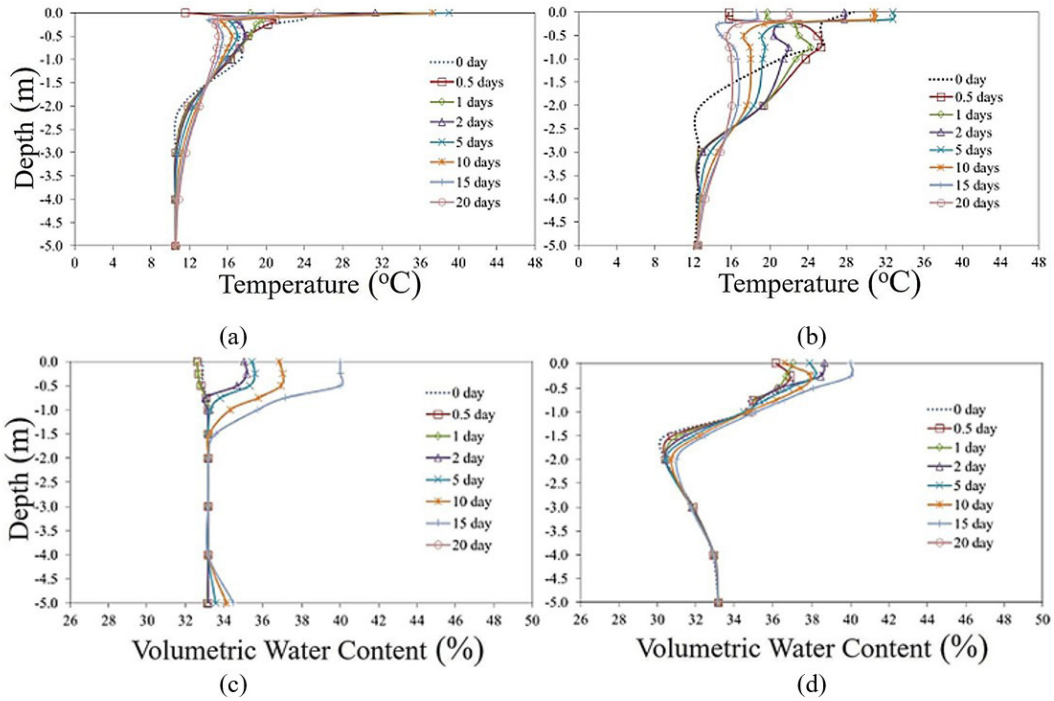

Figure 3. Depth of the active zone based on field monitoring data - (a) and (c) instrumentation installed in a plateau or horizontal plane area; (b) and (d) instrumentation installed at a slope area. Adapted from An et al. (2017).

Complementary and further aspects related to soil-atmosphere interactions, not herein considered, may be found in the works by Boscov et al. (2025), Coutinho et al. (2025) and Gitirana et al. (2025) published in this same issue of the Soil & Rocks Journal.

2. Hydric balance aspects

An extensive review on hydrologic cycles and hydric and energy balances on the earth surface considering soil-plant-atmosphere interactions has been put forward by Borma et al. (2023). Disregarding the important role of vegetation, Equation 1 represents the hydric balance, variable with time, within the soil compartment due to the soil-atmosphere interaction:

$$P = E + FF + RO + Be \tag{1}$$

where: P = precipitation, E= Evaporation, FF = free water flow within the soil mass, which is given by $I + Ss(t\text{-}t_0)$, where I = infiltration and $Ss(t\text{-}t_0)$ = variation in the soil-water stock (or soil-water volume) over time, RO = runoff, and Be = basal or lower frontier water flow.

Figure 4 shows an example of the application of Equation 1 to a soil slope, including associated contour conditions, which are of fundamental importance in any analysis of soil-atmosphere interaction. In this figure, ULF represents the upstream lateral frontier of the problem, usually taken as impermeable in the presence of an unsaturated soil profile, and DLF is the downstream lateral frontier (considered a free flow contour condition in the case). The top frontier (TF) represents a contour condition associated with environmental variations, while the basal frontier (BF) represents the contour condition associated, typically, with a bedrock (or SPT impenetrable depth), which is strongly a function of its potential drainage conditions (impermeable or not), not easily identifiable.

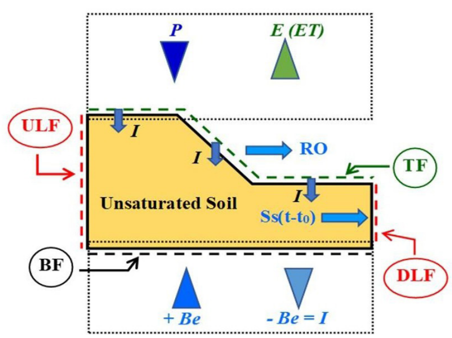

Figure 4. Hydric balance in an unsaturated soil slope as related to boundary conditions.

Regarding Equation 1 (and Figure 4), P and E (or ET=evapotranspiration in the presence of plants) are the main variables usually taken in hydric balances. For instance, if $P\text{-}E > 0$, the site is named as a wet site. On the contrary, if P-$E < 0$, the site is called as dry, which has significant consequences when evaluating geotechnical engineering issues. For example, it is well known that soils, particularly those with a clayey composition, may crack under dry conditions. This aspect is discussed in a subsequent item.

Precipitation (P) data is obtained from local or regional climatic monitoring stations or a net of rainfall monitoring instruments (rain gauges). Evaporation (E) is typically defined using soil-atmosphere interaction equations or theoretical formulations, such as those proposed by Wilson (1990), which require data from climatological stations, not always readily available. It can, however, be estimated by monitoring simple devices installed at a given site (e.g., São Mateus et al., 2012). An empirical alternative to do so is included in what follows.

The term FF in Equation 1 encompasses both rainfall water infiltration in the soil profile (I) and the free water (water that is not retained by soil structure and flows through interconnected soil pores) sub-superficial outflow $Ss(t\text{-}t_0)$, which is given by Equation 2, where t = time, z = depth, S = degree of saturation, n = soil porosity, V_w = water volume.

$$Ss\left(t-t_0\right)=\int_0^z S,n-\int_0^z S_0,n_0=\Delta V_w=V_w-V_{w0} \tag{2}$$

In a first approximation (homogeneous and infinite depth soil), 1D infiltration can be computed using the Green & Ampt (1911) proposal or, in a more rigorous form, based, for example, on Simunek et al. (2005). $Ss(t\text{-}t_0)$ cannot be evaluated separately. Indeed, it is included in the internal water flow analysis, which is conducted according to contour conditions (in conjunction with the infiltration process). For that, extended 2D forms of Green-Ampt (e.g., Fernández-Pato et al., 2018) and, for instance, the Richards saturated-unsaturated flux equation (Richards, 1931) are employed. Solutions for these are currently available in well-known software packages (e.g., FLO-2D, PLAXIS).

The initial water volume (V_{w0}) in Equation 2 is a function of the structure of each soil layer, particularly regarding the mineralogy of its fine fraction (e.g., Mitchell et al., 2025). In geotechnics, it may represent the initial moisture (or associated suction) profile required in numerical analysis. In other application areas, such as agriculture, this term may refer to the amount of water in the subsoil required for vegetation to survive under dry conditions. Some aspects related to defining such initial moisture content profile are discussed in item 4.2.1.

The term RO (runoff or above-ground surface free water flow) is generally taken as given by P - I. It essentially depends on the rate of rainfall water infiltration at a given site, which is limited by the saturated permeability of the upper layer of the soil profile. Lysimeters, associated or not with instrumentation to monitor water moisture and/or soil suction, can be used to evaluate such parcel of the hydric balance at a given site (e.g., Portocarrero et al., 2017, 2021). However, this is not usual, as RO is evaluated based on numerical analysis results that comprise the FF term mentioned above. To do so, apart from contour conditions defining drained (e.g., high permeability zones in the soil profile, free flow at a slope face) or undrained (e.g., sound rock) interfaces in the soil profile under consideration, it is required, at least, the knowledge of the saturated permeability of the materials involved as well of their soil-water retention or soil-water characteristic curve (SWRC - e.g., Fredlund et al., 2012).

The term Be in Equation 1 and Figure 4 represents the amount of water that can enter and be stored in the subsoil (+ Be) or leave it through its basal or lower boundary (- Be). Positive Be implies an upward water flow through fissured bedrock or sound bedrock with interconnected fracture planes, potentially contributing to the formation of a water table at the site, variable with time. Part of this basal inwards water flow may run laterally, contributing to the sub-superficial outflow Ss (t - t_0). Negative Be implies water infiltration through this boundary, which is usually not easy to define and potentially contributes to an increase in the lateral outflow Ss (t - t_0).

2.1 Empirical evaporation assessment

Besides the well-known relevance of infiltration processes in soils, evaporation is an important aspect to be considered in air/atmosphere water exchange problems. An empirical procedure for assessing evaporation in cover layers of solid waste landfills was proposed by São Mateus et al. (2012), who analyzed the water balance at the Metropolitan Center landfill in Salvador, BA. Undisturbed soil samples were collected from the cover layer, and a double evaporation experiment was performed, measuring water loss using two identical vessels under the same atmospheric conditions. One vessel contained the soil specimen initially saturated, while the other was filled only with water. The water reservoir is intended to reproduce potential evaporation conditions (E_p), while the soil reservoir represents the evaporation conditions in the soil cover (E) under the same weather exposure conditions. Based on the experimental results of the evaporation rates in soil (E) and water (E_p), the function E/E_p x θ, the soil volumetric water content, is determined. In this case, the authors successfully employed a linear fitting (Figure 5).

Conceição et al. (2021) used the same procedure as São Mateus et al. (2012) to create a boundary condition modifier function to evaluate the long-term stability of two urban slopes at Salvador-BA. Although present in many geotechnical suites for problem simulation using the Finite Element Method (FEM), the use of evaporation or soil-climate interaction boundaries often requires seldom available or estimated input data. Using this procedure, the soil-climate interaction boundaries are replaced with time-variable boundaries adjusted by modifier functions, which are also present in many geotechnical modeling packages.

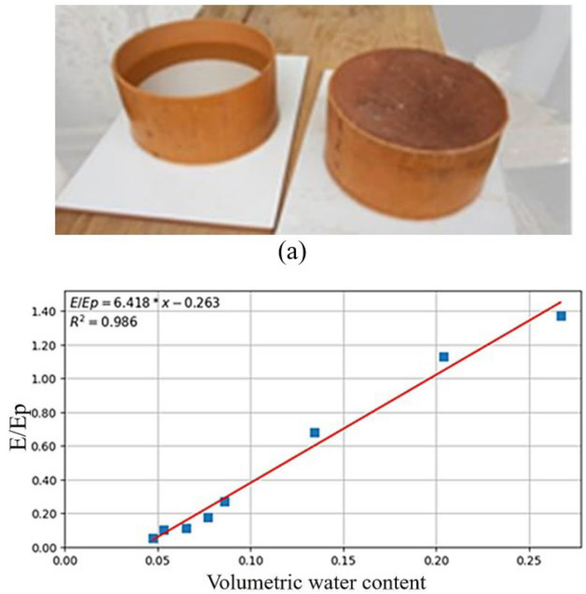

(a)

(b)

Figure 5. (a) double evaporation test for E/EP determination: vessel at left filled with water and, at right, containing undisturbed, saturated soil; (b) linear fitting of the E/Ep data as a function of the cover layer water content. Adapted from São Mateus et al. (2012).

The unity flow (q) boundary conditions are applied to the soil surface, representing rainfall events and potential evaporation for the analysis period. Most modern rain gauges produce rain data on a ten-minute basis, and rainfall data can be imported from the closest weathering station into the slope stability/unsaturated flow program. Furthermore, for potential evaporation E_p, mean daily data are perfectly admissible, and experimental values are usually available. After entering the rainfall ($q > 0$) and E_p ($q < 0$) for the analysis period, the E/E_p function is used as a boundary modifier function, adjusting the evaporation rate as a function of the soil's water content or suction, since in such an analysis the SWRC is required. This empirical procedure has the advantage of applying boundary conditions derived from experimental results obtained using undisturbed soil samples collected from the study area. Figure 6 illustrates a typical modified function for soil-climate interaction. For positive values of pore water pressure, the modifier factor is equal to unity, i.e., no modification is applied in the raining events. However, as evaporation progresses and the soil water content decreases (see Figure 5), the modifier factor assumes progressively smaller values, reducing the evaporation rate at the soil surface as a reflection of the decrease in interstitial water due to matric suction.

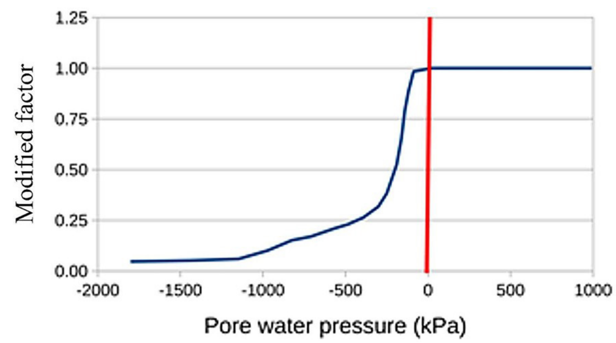

Figure 6. Typical modifier function in terms of pore water pressure.

Among the climate change predictions in the latest IPCC (Intergovernmental Panel on Climate Change) reports, the average global temperature is expected to increase by between 1.8°C and 4.0°C by the end of the 21st century (IPCC, 2023). Forecasts indicate that droughts will be the most severe since those observed in the pre-industrial period in the 19th century. In Brazil, areas susceptible to climate adversity may suffer the most severe implications of these changes, with the most intense droughts likely to occur with an increasingly shorter return time (Cunha et al., 2019; Rocha Júnior et al., 2020).

Consequently, climate-driven processes, such as the appearance of desiccation cracks, are expected to change in incidence and severity over the next 50 years. Furthermore, precipitation values of around 200 mm/h could go from a current recurrence period of 100 years to 10 years, i.e., they would become commonplace. Extremely long periods of drought,

2.2 Cracks formation

One of the consequences of soil-atmosphere interactions is the development of desiccation cracks, which occur due to the wetting and drying cycles to which soils are subjected.

interspersed with intense rainfall, can alter the condition of soils. Fine soils, for example, are prone to cracking during prolonged wetting and drying cycles, which can compromise their integrity and alter their behavior (Li et al., 2016).

Desiccation cracks affect the long-term hydraulic and mechanical behaviour of cohesive soils. Cracks can significantly accelerate water infiltration in clay soils (Mitchell & Van Genuchten, 1993; Zhang et al., 2020), affecting the stability of natural and constructed slopes. Moreover, Gao et al. (2025) state that an increase in crack ratios can significantly reduce the safety factor of a cracked slope compared to an intact slope. Oliveira (2021) also demonstrated the need to include the effect of cracks in stability analysis. After numerical simulations, the author stated that the stability of an unsaturated soil slope subject to rain infiltration can be up to 40% lower in the presence of desiccation cracks compared to the stability of the same slope without desiccation cracks. The factor of safety is lower the greater the depth of cracked soil.

Some of the impacts on soil are difficult to determine and may be influenced by multiple soil-climate interaction processes. When exposed to high temperatures, soils undergo volume changes that can cause desiccation cracks. The cracks begin when the tensile strength of the soil is exceeded by tensile stresses induced by the drying process.

Experiments have already been carried out to understand the mechanisms of initiation and propagation of desiccation cracks (Levatti et al., 2019). Various test methods have been employed to measure the behaviour of crack-prone soils, such as triaxial testing, flexural testing, hollow cylinder, unconfined penetration, etc. (Vanicek, 2013).

Cui et al. (2013, 2014) described a large-scale environmental chamber developed to conduct desiccation tests on reduced models. The authors realized that in the clay soil studied, which was initially compacted, cracks began when the soil had a high volumetric moisture content (60%). The evolution of the number of surface cracks and the average crack width was considered very consistent, indicating that only one of the two parameters is needed to analyse the influence of soil cracking on soil-atmosphere interaction.

Tang et al. (2011a, b) employed image processing techniques to monitor crack development in three soil samples subjected to drying. A Soil-Cracking Ratio (R_{sc}), which is the ratio of the surface area of cracks to the total surface area of a soil sample, was defined to quantify the crack extension at the soil surface for different gravimetric water content. Figure 7 illustrates the evolution of R_{sc} with respect to the moisture content during drying.

R_{sc} increases while water content decreases at the early cracking stage. Conversely, as the drying process continues, the growth in R_{sc} starts to drop when the water content approaches the air entry value (AE point). After the water content reaches a transition point corresponding to 9.5%, which is actually identical to the shrinkage limit (*SL*) determined from the shrinkage curve (Tang et al., 2011b), further water loss does not result in any additional increase in R_{sc}. This indicates that cracks have approached stabilization. Figure 7 also shows that almost 90% of cracks were well-developed before the water content reached the AE point.

In addition to wetting, which can cause cracks to close, very high temperatures can also cause the soil to self-heal the desiccation cracks once the soil has already reached its shrinkage limit. At a temperature of 105°C, Hedan et al. (2012) found that desiccation cracks were no longer observable and appeared to have closed. The healing process was interpreted as a thermally driven process, i.e., a thermal dilatation of the water and the clay minerals after the shrinkage limit was reached. This could lead to a gradual closure of desiccation cracks. Thus, it is understood that both forms of volume variation can occur during extreme drying processes. Firstly, contraction is induced by high suction, and once the soil's contraction limit has been reached, expansion is induced by high temperatures (Di Donna & Laloui, 2015).

Cracking evolves not only on the soil's surface but also at depth. Miller et al. (2016) propose a theoretical equation for determining the depth of desiccation cracking (Equation 3).

$$Z_c = \frac{E}{K_0 \gamma H (1-\mu)} \Delta(u_a - u_w) + \frac{\sigma_t}{K_0 \gamma} \tag{3}$$

where: Z_c is the depth of the crack, E is the modulus of elasticity corresponding to the effective normal stress, K_0 is the ratio between the total horizontal and vertical stress before the desiccation process, γ is the total specific weight, H is the modulus of elasticity related to suction, μ is the Poisson's ratio, $\Delta(u_a - u_w)$ is the variation in matrix suction and σ_t is the tensile strength of the soil. As an example, this calculated crack depth can be related to the wetting front depth observed in field experiments.

Desiccation cracking can severely impact the performance of clay soils in various geotechnical, agricultural and

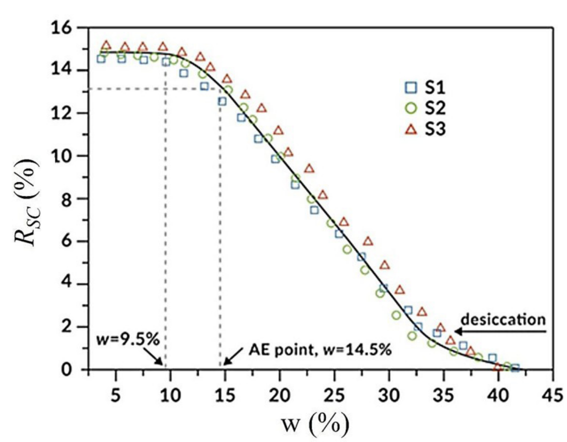

Figure 7. Evolution of crack intensity factor with moisture content during drying (Tang et al., 2011a).

environmental applications. In geotechnics, the presence of desiccation cracks can reduce the stability, hinder maintenance and impair the hydraulic performance of earth structures (Kodikara & Choi, 2006). This is because cracking on the surface of soils increases the infiltration rate of rainwater (Anderson et al., 1982; Zhan et al., 2006; Rouainia et al., 2009). On the other hand, cracking indicates the development of a perched layer with extremely low unsaturated permeability that inhibits water transmission from the soil to the surface where evaporation occurs.

Understanding the effects of micro- and macro-scale cracking on the hydraulic and mechanical behaviour of slopes is fundamental if the impacts of climate change on slope stability are to be assessed. The development of cracks in soils has been studied in the laboratory, but the prediction of crack development in field conditions, where a greater number of variables need to be considered, such as wetting and drying variations, root reinforcement, preferential surface drainage paths, etc. is still little studied (Tang et al., 2018).

Because of their low tensile strength, cracks can occur when the value of the thrust coefficient K_0 approaches zero and the tensile strength is reached. Figure 8 illustrates a conceptual model of tensile cracking in the unsaturated zone, which occurs at a depth where K_0 is zero or negative (Lu & Likos, 2004). This at-rest coefficient of earth pressure, K_0, corresponds to the definition by Fredlund (1979), which is the ratio of the horizontal to the vertical net stresses. As discussed by de Campos et al. (2021b), such a value of K_0, which can be seen as given in terms of total stresses, is smaller than that defined in terms of Bishop's effective stresses (Bishop, 1959). Regardless of its definition, K_0 will vary with the soil profile moisture content (and thus, suction) under climate changes. Thus, the depth of tension cracks might vary according to variations in temperature and rainfall conditions at a given site, and, in agreement with Equation 3, the lower the soil moisture content (and higher its suction), the deeper the soil tension cracks.

Fredlund et al. (2010) used a continuum mechanics approach to formulate unsaturated hydraulic conductivity functions for fissured clay soils. The characteristic curve and permeability function they found take a bi-modal form. They discuss the impact of various levels of surface cracking on soil suction distributions.

Li et al. (2011) developed a method for predicting the characteristic curve and permeability function of cracked soil, considering the volume variations of the cracks during the drying and wetting processes. Cracked soil is seen as a superposition of a network of cracks on a soil matrix. The cracks are considered a series of known geometry pores in different states. The authors utilize the pore size distributions of the two systems (cracks and matrix) to estimate the retention curve and the permeability function. The functions associated with the two systems are then combined to determine the functions corresponding to the fissured soil. Abbaszadeh et al. (2015) also concluded that the characteristic curve of fissured soils has a bimodal shape.

Li et al. (2011) monitored the development of cracks in soils in the field. They concluded that except when considering that the cracks did not vary in volume, the characteristic curve of the cracked soil is not substantially affected by the presence of cracks. On the contrary, the permeability coefficient is significantly affected by the presence of cracks and can be 3 to 100 times greater. The permeability function is bimodal when the cracks are open under saturated conditions. The crack network dominates permeability at low suction levels, but the soil matrix controls permeability at high suction levels. The saturated permeability prevails in the soil matrix when the cracks close completely under saturated conditions. If cracks appear later at low suction, the permeability in the low suction range can be dominated by that of the crack network.

The soil matrix also controls permeability at high suctions because water is retained in cracks with large openings. When cracks close under saturated conditions and open at high suction, the permeability function of the cracked soil is similar to that of the soil matrix.

According to Novak et al. (2000) and Mitchell & Van Genuchten (1993), the infiltration capacity of soil without cracks is less than half that of soil with cracks.

In turn, the soil suction profile depends on the initial suction of the soil surface. According to Fredlund et al. (2010), the results depend mainly on whether the initial matric suction is lower or higher than the air entry value in cracked soil. The variation in the soil's matric suction increases with the increase in the volume of cracks. When

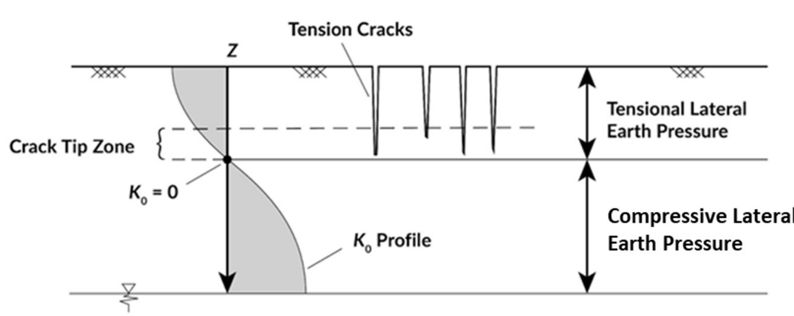

Figure 8. Development of tension cracks in unsaturated soil (Lu & Likos, 2004).

substantial cracking occurs in the soil, the matric suctions are uniform along the soil's surface. The same behaviour is observed if the initial suction is higher or lower than the air intake value of the cracked soil.

Soil surface matric suction increases during evaporation and decreases during infiltration in bare soil regions. When cracks occur in the soil, and the suction along the surface is lower than the air intake value of the cracked soil, the matric suction can increase or decrease during infiltration conditions. This behaviour depends on the magnitude and distribution of the matric suction along the depth.

3. Erosion processes

In the context of soil-atmosphere interaction, erosion processes – whether geological or accelerated by anthropogenic actions – emerge. They can be classified as either wind or water erosion in tropical environments. Wind erosion, a topic little explored in the Brazilian literature, is generally superficial. In contrast, water erosion is categorized as internal (piping and eluviation) and superficial (sheet erosion and splash erosion caused by raindrops), resulting in the formation of grooves, gullies, and ravines. Gullies and ravines may take on linear, curved-linear, or amphitheater-like shapes.

As outlined by Primavesi (1952), the balance and stability of soil in the face of erosive processes are directly related to the soil biology conditions. Soil biology is influenced by environmental conditions, which are frequently impacted by human activities such as land use and occupation, the introduction of contaminants, and the application of chemical compounds in the soil, water, or air. These actions can lead to the extinction of certain species. It is worth emphasizing that land occupation and use can also impact the temperature of the soil mass, affecting not only the organisms within it but also its hydro-mechanical behavior.

With the expansion of agribusiness and disorderly urban occupations in Brazil, wind erosion has reached significant proportions. However, this topic remains underexplored in the national literature and requires further study. However, anthropogenic water erosions are the focus of the discussions presented here. In agricultural areas, both wind and water erosion acting on the soil surface has intensified significantly in Brazil, with little attention given to the desertification processes they cause, which are accentuated by internal water erosion. Water erosion originating from agricultural areas is also largely responsible for the siltation of watercourses and reservoirs, as evidenced by Sales et al. (2024). In geotechnical contexts, attention is generally focused on anthropogenic gullies and ravines, which pose immediate threats to infrastructure and human lives.

The occurrence of different types of water erosion in tropical environments, such as those found in Brazil, depends on the specific circumstances under which they arise and their direct relationship with soil-atmosphere interactions. These interactions are, in turn, influenced by geology, geomorphology, the characteristics and behavior of weathering profiles, climate, microclimate, land occupation, and soil use. It is essential to recognize that occupation and land use directly impact both climate and microclimate, significantly contributing to landscape dynamics.

In this text, the term "microclimate" refers to regional and local climates, as Camapum de Carvalho et al. (2024) highlighted. This differs from Primavesi's (1952) use of the term, which focuses on the soil's surface layer. Climate and microclimate are closely linked to rainfall, variations in atmospheric and soil temperatures, relative humidity, terrain morphology, wind direction, and solar radiation (Luiz et al., 2012). These factors directly influence erosive processes and interactions between the soil and atmosphere.

The topic of water erosion in tropical environments, particularly in geotechnical contexts, has been extensively addressed in Brazil through booklets (Camapum de Carvalho & Diniz, 2007; Camapum de Carvalho & Lelis, 2006; Ribeiro et al., 2016; Camapum de Carvalho et al., 2016), books (Camapum de Carvalho et al., 2006; Loureiro & Guerra, 2023; Primavesi 1952; Sales et al., 2017, 2024), dissertations and theses, national scientific events (National Symposium on Erosion Control, Brazilian Conferences on Unsaturated Soils and on Environmental Engineering) and regional scientific events (Symposia on Tropical Soils and Erosive Processes in the Midwest), as well as various articles published in Journals.

This text provides a comprehensive discussion of the primary types of water erosion in geotechnical contexts, highlighting key points that have contributed to understanding the phenomenon and identifying aspects that warrant further study, particularly regarding the impacts of soil-atmosphere interactions.

3.1 Superficial erosion and grooves in the context of soil-atmosphere interaction

Surface water erosion caused by the impact of raindrops and laminar water flow has been occurring on a large scale. This phenomenon results from land occupation and use, whether in urban or rural environments, and almost invariably involves significant human activity. Often, insufficient attention is paid to the negative effects of occupying spaces and using the land. Typically, the impact of raindrops causes soil particles to detach and splash, with the erosive process further intensified by the flow of surface water.

Primavesi (1952) provides a historical overview, highlighting situations from ancient times to today where surface erosion has led to soil degradation and desertification, underscoring the need for greater attention to these issues. Regarding erosion that affects agricultural production, the author extensively discusses internal erosion, which significantly contributes to the loss of soil productivity. In the geotechnical field, internal erosion impacts the properties and hydromechanical behavior of the soils (Lima, 2003).

In urban areas, the execution of construction projects and the establishment of housing developments without proper planning and necessary precautions are among the leading causes of surface erosion. Added to this is the impact of microclimatic changes caused by urban development, which directly affects the interaction between soil and the atmosphere.

In rural areas, particularly in agricultural zones, improper management and the use of chemical fertilizers contribute to the occurrence and/or intensification of surface erosion. These factors are compounded by changes in soil-atmosphere interactions, which alter flow and infiltration conditions, as well as precipitation regimes. Pérez & Camapum de Carvalho (2023) and Camapum de Carvalho et al. (2023) analyzed a tropical weathering profile typical of the Federal District of Brazil, showing that certain mineral inputs used in agriculture not only facilitate soil disaggregation but also affect suction and mechanical behavior, thereby influencing laminar erosion processes. It is worth noting that chemicals introduced into the soil can migrate, causing eluviation within the soil mass, which promotes erosion and alters interparticle forces, potentially leading to mass instability.

Soil disaggregated by agricultural inputs and wetting-drying cycles forms an impermeable surface layer that increases surface runoff. Momoli et al. (2017) emphasize that water movement through soil, rock, or on the surface forms part of the hydrological cycle, which can lead to erosive processes and/or eluviation. In this context, the interaction between soil and atmosphere plays a significant role.

Grooves form due to concentrated water flow in urban or rural environments. An aspect that warrants further investigation is the impact of transversal water energy on their formation and evolution. An example of that is sea waves moving inwards and outwards on a clean sandy beach site. As the water from a wave moves outward, the main movement direction is perpendicular to the beach. However, transversal seawater movements also occur, contributing to the formation of grooves, as shown in Figure 9.

3.2 Ravines and gullies in the context of soil-atmosphere interaction

There are different criteria in the literature for classifying erosions as ravines or gullies, as Camapum de Carvalho (2023) noted. Guerra (1998), for example, considers gullies to have depths and widths greater than 50 cm, and ravines to be below this limit. Camapum de Carvalho et al. (2001) associate the distinction between ravines and gullies with the stability of the slopes, indicating that when the slopes become unstable, erosions can be classified as gullies.

Camapum de Carvalho (2023), when addressing the theme "*Erosion in the Cerrado from different perspectives*", considers that the predominant shapes of ravines and gullies are amphitheater, linear longitudinal, and curved longitudinal. In tropical environments, the shape of ravines and gullies is generally influenced by geology, geomorphology, weathering profile characteristics, and surface and subsurface flow conditions. Almost always, ravines and gullies result from an evolutionary process starting with surface erosion and the formation of grooves. However, they are not infrequently caused by the improper placement of drainage systems' discharge and the exploitation of soil borrow sites, as in the case studied by Ramidan et al. (2013), discussed next. A particular situation is presented by Araujo et al. (2018), who identified vegetation removal and irregular cuts in slopes as factors that exacerbated the ravines and gullies caused by rainfall in the Arlindo Cavalcante neighborhood, Bonito, PE. It should also be noted that urban occupations tend to interfere with the microclimate within the massif, making it susceptible to mechanical behaviour instabilities in the soil, particularly when combined with the infiltration of chemically polluted fluids.

In flat regions, such as Brazil's Cerrado and other regions of the Country with smoother topography, erosion typically takes on a linear shape and, in some cases, a curved shape. However, when located at the edges of plateaus and areas with greater slopes, they often assume an amphitheater shape, as illustrated in Figure 10a, almost always originate from slope

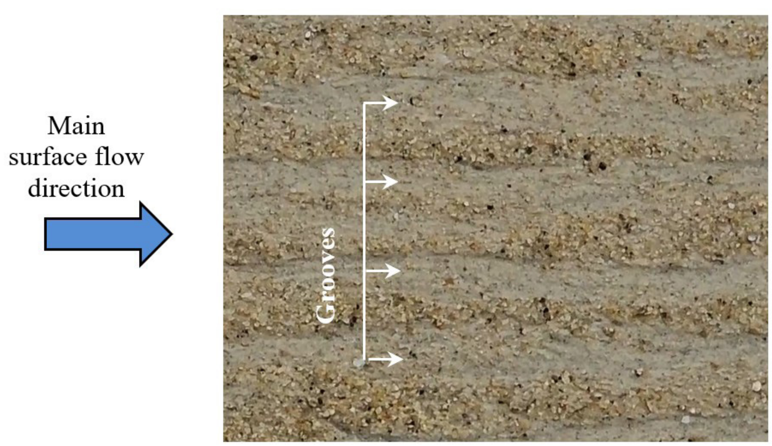

Figure 9. Grooves shaped on a beach sand, with channel formation being also a function of transversal water movement.

failures. This type of erosion is also common on reservoir margins, where an increase in water content at the base of the surrounding slopes and plateau edges, sometimes coupled with the undermining of the slope base, causes slope failure that progresses into amphitheater-shaped erosion. Today, with the increase in the volume of river courses, the expansion of margin erosion that does not fit the classic erosion models of ravines or gullies is becoming more pronounced

(Figure 10b). A further erosion shape occurring under specific geological and/or geomorphological conditions is exemplified in Figure 10c. This erosion shape, named herein as with a diffused shape, originates from the diffused flow of surficial rainfall water over an erosion-resistant superficial unsaturated material underlead by a silt-sandy or sand-silty erodible one. Such erosion shape has some similarities with that exemplified in Figure 10b. It differs, however, by not resulting from any water flow at the toe of the plateau and/or failure of the topsoil by fall or topple.

Camapum de Carvalho (2024) considers that the triggering and amplifying factors of erosive processes can be internal, interface, or external. The onset and evolution of ravines and gullies frequently involve a combined action of two or more internal and external factors. In this context, understanding the phenomena at both micro and macro scales is relevant for erosion control and the recovery of eroded areas.

According to Camapum de Carvalho (2024), internal factors comprise the soil profile, including geological characteristics, hydrogeology, subsurface geomorphology, soil type, and the quality of the fluid present. The surface geomorphology is considered an interface factor, and its relevance is analyzed by Jesus et al. (2023), who account for variations in tension and water content in the soil profile, with water content resulting from interactions between the soil and atmosphere. The author classifies external factors into natural and anthropic. The natural factors include the sun, wind, and rain, which significantly impact the soil-atmosphere interaction and significantly influence flow in saturated and unsaturated media. Anthropic factors, such as land occupation and use, ultimately influence the microclimate.

In the pursuit of understanding the influence of soil-atmosphere interaction on the evolutionary process of ravines and gullies, the process of eluviation, along with the slopes resulting from flow in both saturated and unsaturated media, emerges as a highly relevant factor, as shown by Lima et al. (2017). With eluviation, the soil's resistance is reduced, leading to slope ruptures on the margins, which in turn expand the ravine or gully, depending on the case. In addition to the eluviation of the soil, undermining the slopes' bases when precipitation water flow is channeled often plays a role in the rupture mechanism of ravine and gully slopes (Camapum de Carvalho et al., 2006). Lima et al. (2017), in their study of amphitheater-shaped erosions in the Manaus region, found that cracks resulting from neotectonics movements favored the evolution of the erosions through the destabilization and fall of blocks.

3.3 A case study example

In soil-atmosphere interactions, the predominant factors in both environments are of considerable importance. Atmospheric factors include relative humidity, temperature, sunshine and wind, with its characteristics of speed and direction. In the soil,

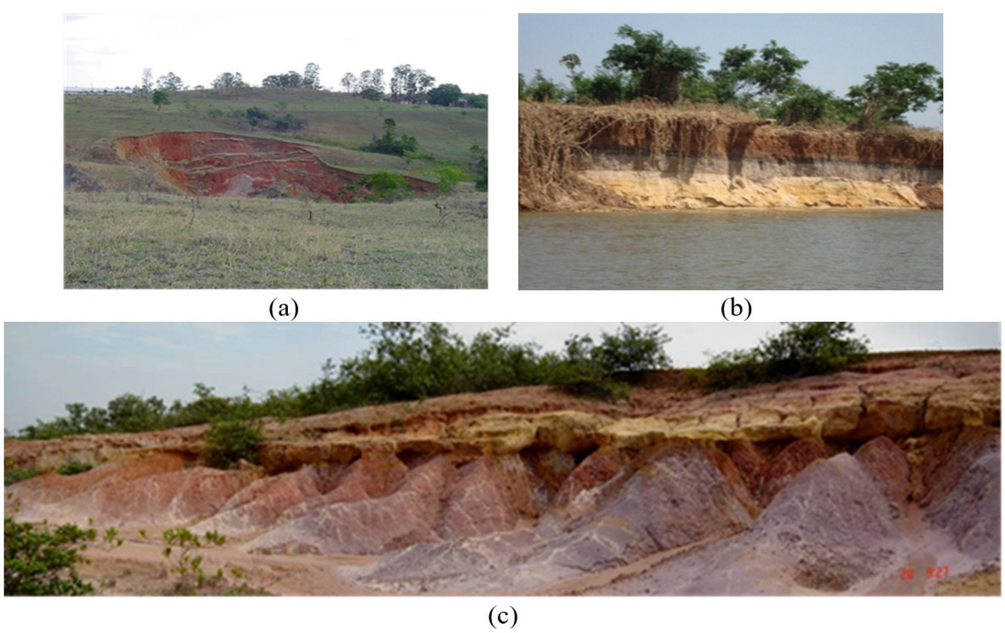

Figure 10. (a) amphitheater-shaped erosion in Anápolis, GO; (b) erosion on a bank of the Araguaia River, Goiás; (c) erosion of a cut slope (Barreiras Formation) in the Galeão Airport in Rio de Janeiro, RJ (Portocarrero, 2009).

for example, its physical properties, chemical-mineralogical composition, and the suction acting on it, as a result of humidity and porosity, are important (e.g., Portocarrero et al., 2021). Thus, in addition to the quality of rainwater and/or surface/subsurface water, several factors interfere with soil-atmosphere interaction and, consequently, with the onset and evolution of erosion processes (e.g., Luiz et al., 2017).

Ramidan et al. (2013) give an example of the role of these interactions. They present the case of pluvial erosions resulting from the exploitation of a borrow area for constructing an earth dam in the Brazilian Central Plateau, leading to the setup of gullies and downstream silting processes, as exemplified in Figure 11.

This case of pluvial erosion with anthropogenic origins provides a good example of the relevance of soil-atmosphere interaction in the continuous development and evolution of erosion processes. Indeed, the reported analysis shows that such interaction begins with the formation of the weathering profile, a long-standing process. At the site, after the removal of some 4 m to 5 m of cover soil for the embankment construction, the unsaturated soil profile comprised a superficial, colluvium layer of a lateritic material (formed by translocation of iron and aluminum oxides from the previously existing soil cover), followed by a mature residual soil layer and two layers of saprolitic soil of biotite-gneiss origin (A and B), with the lower layer (B) being less weathered. The ground gradient was low, averaging approximately 2%. The water table, with its baseline probably related to the earth-dam reservoir, was at an average of 13 m below ground level.

Besides conventional physical-chemical-mineralogical characterization tests, the local materials were identified through mini-MCV tests (Nogami & Villibor, 1981, 2003; Marinho et al., 2020) and soil-water retention curves (e.g., Fredlund et al., 2012). Susceptibility to erosion of the involved materials was investigated through double sedimentation tests and disaggregation tests (using unconfined cubical undisturbed specimens), as well as Inderbitzen (to evaluate laminar or surficial erosion) and pinhole tests (to evaluate piping erosion), refer to Ramidan (2003) for details. The tensile strength of the materials (a non-conventional but promising testing method

for evaluating erosion potential in soils (e.g., Araujo & de Campos, 2013) was also determined. As a result, the residual mature soil was identified as the highest erosion-susceptible material, followed by saprolitic soil A, saprolitic soil B, and colluvium (lateritic) soil.

In line with the subject of the present contribution, Figure 11 shows part of the area exposed, and part covered by vegetation, both of which are affected by soil-atmosphere interaction in different ways. During periods of drought, the area covered by vegetation tends to increase soil evaporation (through evapotranspiration), while under rainfall, it enhances infiltration and minimizes surface runoff. The opposite is expected in the area without cover. During the dry season, the unprotected soil is subjected to increased suction, allowing the air phase to remain continuous within the massif. During the rainy season, rainfall triggers the phenomenon of splashing, which promotes the desegregation and detachment of soil particles. This is followed by the formation of a sheet of water, causing infiltration to occur under high suction. Besides the development of surface erosion by runoff, a saturation front develops, accompanied by a concomitant decrease in the suction (and associated strength) of the sub-superficial material. It cannot be disregarded that a potential occurrence of a Lisse-type effect (see item 5.2) may contribute to the desegregation of soil clusters during the rainwater infiltration process into the unsaturated soil profile. Nonetheless, it is clear that the initial state of soil hydration, which is a function of soil-atmosphere interaction, plays a crucial role in the development of surface erosion.

The potential process of surface soil contraction due to an increase in suction in dry periods and compaction

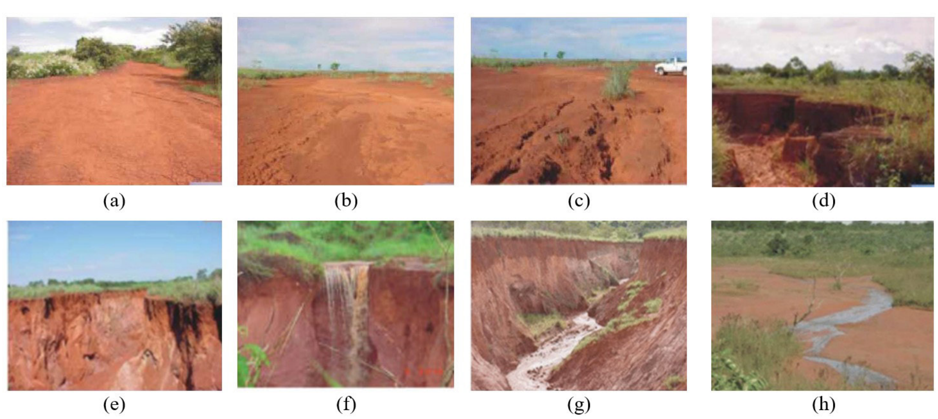

Figure 11. (a) area exposed to surface erosion by raindrops fall and groove formation; (b) micro-rills formation; (c) beginning of ravine formation by concentrated water flow; (d) end of evolution of the erosive process by ravine; (e) gully head formation; (f) gully formation from concentrated superficial water flow; (g) gully development including underground water contribution; (h) downstream siltation. Adapted from Ramidan (2003).

of the exposed soil under the energy of raindrops may generate portions and veins of topsoil with greater hardness and, together with the variation in the transverse energy of the water in the surface flow, the appearance of furrows (Figures 11a and 11b).

According to Ramidan et al. (2013), the gullying processes observed at the site in the case under analysis were caused by the flow of surface water resulting from rainfall (Figures 11e and 11f). It should be noted, however, that after the formation of ravines and gullies (Figures 11c and 11d), the continued action of soil-atmosphere interaction generates the degradation of the massif near the slopes through flow in an unsaturated condition, facilitating its rupture and the evolution of erosion (Lima et al. 2017), a process amplified in this case by the occurrence of groundwater flow (Figure 11g). Even in the case of groundwater flow, this depends on soil-atmosphere interactions and the microclimate associated with them, which directly influence the processes of precipitation and rainwater infiltration in the soil profile.

Going towards the final phase of the processes as a whole, the resulting silting process (Figure 11h), the transported eroded soil, when deposited in a flat area, has its resistance increased during dry periods, making it able to receive new layers of eroded soil without part of it undergoing surface erosion processes. Alternatively, it may contribute to silting lakes and rivers, promoting further environmental degradation impacts not considered herein.

4. Slope stability

The combination of tropical soil profiles, commonly consisting of unsaturated residual and colluvial soils, associated with mountainous environments and high precipitation rates, creates favorable conditions for the occurrence of gravitational mass movements (e.g., de Campos et al., 2018). A frequent cause of slope failures is associated with periods of precipitation, which promote water infiltration into the unsaturated soil (e.g., Lumb, 1975; Brand, 1985), leading to a reduction in soil strength due to the decrease in matric suction (e.g., Ching et al., 1984; de Campos, 1997; Rahardjo et al., 2005). In this context, the effects of climate change play a crucial role, as they modify the patterns of the hydrological cycle (IPCC, 2021), particularly, as highlighted by Hobeichi et al. (2022a), in relation to drought.

Considering specific aspects related to slope stability analysis, the role of initial porewater pressure acting in the slope and the effects of extreme drying on the shear strength of the materials involved are considered relevant and discussed below.

4.1 Overview of climatic changes effects

Effects of climate change have become increasingly evident, leading to an increase in the frequency of landslides in various regions of the world, which requires a review of management approaches for such phenomena (e.g., Dehn et al., 2000; Crozier, 2010; Gariano & Guzzetti, 2016; Haque et al., 2019). For example, extrapolations based on past observations of rainfall-induced landslides are no longer suitable for predicting future performance (Dijkstra & Dixon, 2010). Indeed, although the total rainfall global precipitation volume remains relatively constant, regional effects (rainfall distribution) differ significantly, with notable increases in precipitation intensity, duration and changes in frequency (e.g., Trenberth et al., 2003; Groisman et al., 2005; Min et al., 2011; Trenberth, 2011; Westra et al., 2014; IPCC, 2021).

Apart from accentuating extreme precipitation, climate change also accentuates the occurrence of severe droughts (Westra et al., 2014; Adler et al., 2014). Indeed, global warming, besides promoting soil drying with the recurring potential for crack development, contributes to increased evaporation and higher atmospheric humidity levels. Thus, it also intensifies precipitation events (Trenberth et al., 2003). Furthermore, the increased occurrences of extreme precipitation and droughts are also influenced by natural meteorological phenomena, such as El Niño and La Niña, in Brazil (Haylock et al., 2006).

Hobeichi et al. (2022b) reviewed several studies on the impact of climate change on the hydrological cycle, revealing spatially complex trends in water balance components. Their findings indicate that evapotranspiration and runoff show the most significant alterations, while precipitation exhibits the least.

4.2 Aspects related to slope stability analysis

In unsaturated soil profiles, slope stability analysis is typically performed in terms of effective stresses. Thus, apart from aspects related to the stress-strain-strength characteristics of the materials involved (e.g., Tang et al., 2018), knowledge of pore-water pressure distributions is of primary interest. In this sense, slope stability analyses are heavily influenced by climatic and hydro-geological conditions, which determine the variation in pore water pressures and water table fluctuations, particularly in regions with distinct wet and dry seasons (e.g., Cai & Ugai, 2004; Rahardjo et al., 2010; Rahimi et al., 2011). In the presence of a dynamic environment, such as that associated with climatic changes, the assumption of stationary behavior cannot be made (Dijkstra & Dixon, 2010), as it is relevant to assessing the water balance (or suction) within the soil slope. Understanding this dynamic is crucial for determining the pore pressure state of a soil slope in stability analyses (e.g., Iverson, 2000; Gitirana, 2005; Elia et al., 2017).

Assessing *in situ* pore pressure conditions represents a significant challenge, mainly due to the scarcity of slopes with continuous monitoring. This makes the pore pressure state unknown in most cases. Even when slopes are densely monitored, hydrological conditions still present limitations in understanding. The role of climate, particularly precipitation characteristics, is widely recognized as one of the primary triggers for landslides and is, therefore, commonly incorporated into landslide studies. However, several studies, whether comprising retro-analyses or numerical simulations of future behaviour, often disregard the initial state of pore pressures rigorously (e.g., Cai & Ugai, 2004; Gerscovich et al., 2006; Rahardjo et al., 2007). Typically, the "initial" pore pressure state is assumed based on a stationary analysis or simplified distributions such as triangular profiles or pore pressure/moisture constants along the depth. Subsequently, the transient flow analysis simulates the weather conditions for a certain period of time. However, many authors emphasize the importance of a more realistic and representative consideration of the "initial" pore pressure state in analyses (e.g., Toll et al., 2001; Gitirana, 2005).

4.2.1 On the evaluation of the initial porewater pressure distribution

Two evaluations of the "initial" pore-water pressure state in the soil, required in transient analysis in unsaturated soils, are exemplified herein.

The first evaluation refers to transient back analyses performed by Gomes (2019), which were designed to assess failure mechanisms associated with the rupture of a typical granitic-gneiss soil slope profile found in Rio de Janeiro. The study's primary objective was to determine the numerical analysis period required for the effect of the "initial" pore pressure state to become negligible in the stability analysis results. Flow and stability analyses, as well as modeling, were performed using the software package developed by SoilVision. Figure 12 shows the slope boundaries and precipitation conditions considered in that study, as well as the average hydro-mechanical properties of the materials involved. Further laboratory-determined soil properties related to the unsaturated soil profile can be found in Oliveira (2013) and Gomes & de Campos (2022).

Considering the soil-atmosphere interactions prevailing at the time in the site, and assuming that the adopted hydro-mechanical properties did not vary with time, the analysis by Gomes & de Campos (2022) indicated that landslide mobilization predominantly occurs in the superficial layer of the soil profile (mature soil), and that a minimum of an 8-month numerical simulation period is sufficient to reduce the influence of the "initial" pore pressure state hypothesis (constant and triangular distributions) on the analyses. Additionally, the authors verified that the occurrence of saturation at the toe of the slope and its resulting outflow did not influence the stability analysis results, probably due to the larger values of ϕ' and ϕ^b associated with the saprolitic soil layer. This indicates the need to carefully evaluate both flow and shear strength conditions associated with boundary features when attempting to understand failure mechanisms leading to the rupture of natural slopes resulting from atmospheric events.

A second example of evaluating the "initial" porewater pressure distribution considers the effects of climate change in numerical analysis simulations. Following concepts of Geographic Climatology put forward by Zavattini & Boin (2013) and Silva Junior (2015) considered that the climate presents cyclical behavior, as does the water table in a given soil profile. The approach characterizes data from climatic years, with a minimum of 21 years, distributed into three groups based on the quartiles of the total volume of precipitation: habitual, atypically dry, and atypically wet. The habitual climate year represents a situation in which the volume of rainfall is close to the annual historical average. Thus, it denotes the situation in which the amount of water present in the slope represents a situation close to the "initial" pore pressure (or water content) state, making it possible to use it as a starting point in transient analyses.

It is worth noting that the simulation of the "initial" pore pressure state should ensure a null water mass balance when repeating the same climate year in long-term numerical analyses. Indeed, analyses of soil-atmosphere interaction

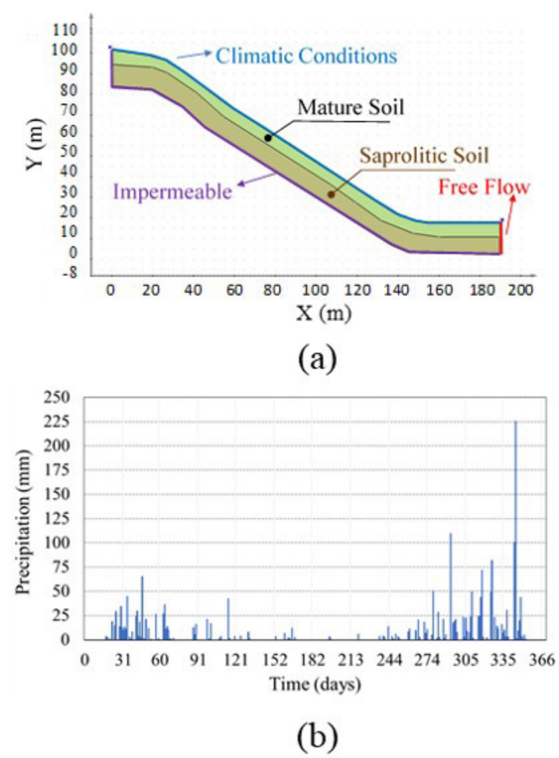

Soil	k_{sat} cm/s	c' kPa	ϕ' degree	ϕ^b degree
Mature	4.50E-03	2.70	26.00	13.00
Saprolitic	1.00E-04	0.00	36.70	18.40

(c)

Figure 12. (a) slope soil profile with boundary conditions; (b) periods of rainfall and soil evaporation previous to landslide setup (modified from Gomes & de Campos, 2022); (c) average hydro-mechanical soil properties (Gomes, 2019).

models, which consider only precipitation and evaporation (or evapotranspiration), tend to generate imbalances in the mass balance. In short-term studies, as illustrated in the above example, these imbalances cause minimal disturbance to the mass balance. However, in long-term simulations, these effects may become significant. This imbalance can lead to two distinct scenarios: when the mass balance is positive, $P - ET > 0$, the model tends to saturation, and when $P - ET < 0$, the model tends to dry out. Also, during intense precipitation events, excess water becomes runoff (*RO*) and is removed from the model when the maximum infiltration capacity of the topsoil is exceeded. Nonetheless, even considering representative boundary conditions, adjusting the mass balance to be suitable for long-term numerical analyses is only possible with the inclusion of basal flow (*Be*), referring to Equation 1 and Figure 4.

Considering the above, Figure 13 shows basic information related to the numerical simulations regarding, in this case, initial pore-water-pressure profile evaluations related to climate change effects. In these simulations, climate data (1997-2021) from an INMET (Brazilian Institute of Meteorology) station in the Região Serrana of Rio de Janeiro were used. Dry, wet, and habitual rainfall conditions were defined based on lower, higher, and average annual rainfall conditions. In the analyses performed, it was assumed that any formation of positive pore pressure at the basal boundary condition [boundary (4) in Figure 13] would result in the removal of excess water volume from the model. Additionally, it was assumed that local hydrogeological conditions, soil hydraulic properties, and the mechanical properties of the soil remain unchanged throughout variations in climate.

Figure 14 illustrates the variation in the average volumetric moisture content [θ_m] and the adopted critical rainfall condition over a 4-year analysis period. As can be seen, the slope θ_m presents a behavior similar to a cyclic sine function (indicated by the broken lines). Additionally, from the third year of numerical simulation onwards, the results tend to converge toward an expected equilibrium condition for stored water. Therefore, for soil-atmosphere interaction analyses, it is recommended that simulating at least two years of habitual climatic data is necessary to achieve an "initial" pore pressure state.

Going further, Figure 15 shows the results of flow and limit equilibrium stability analysis comprising a habitual climatic year (H – black line - total volume of precipitation of 1,683.4 mm), a dry year (D – red line - 1,366.3 mm of rainfall), and a wet year (W – blue line - 1,947.3 mm of precipitation). The upper part of Figure 15 presents the mean volumetric water content variation, and its lower part shows the variation of the safety factor for the three conditions, with an analysis recurrence of every 10 days.

The results indicate that the variables analyzed follow a cyclical pattern, represented by dashed lines, showing periodic behavior over time. It is observed that the dry climate year had little impact on stability conditions, which

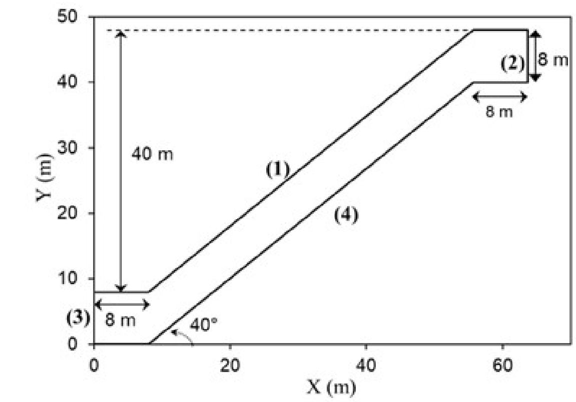

(a)

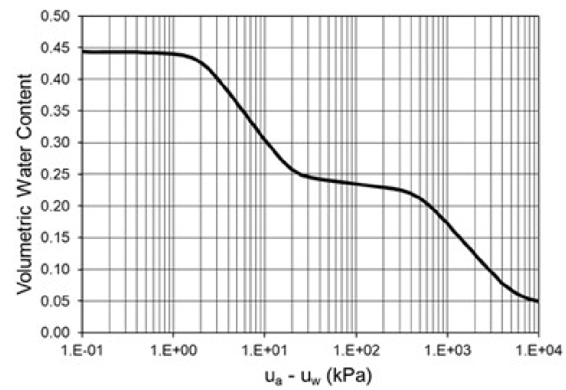

(b)

k_{sat} (m/s)	c' (kPa)	ϕ' (degree)	ϕ^b (degree)	n
$1x10^{-6}$	20	30	15	0.44

(c)

Figure 13. (a) soil slope configuration - numbers within brackets represent boundary conditions as follows: (1) climatic boundary - atmospheric interaction, (2) impermeable, (3) free water outwards flow, (4) semi-permeable boundary, with no permanent water table formation; (b) soil water retention curve; (c) hydro-mechanical soil properties.

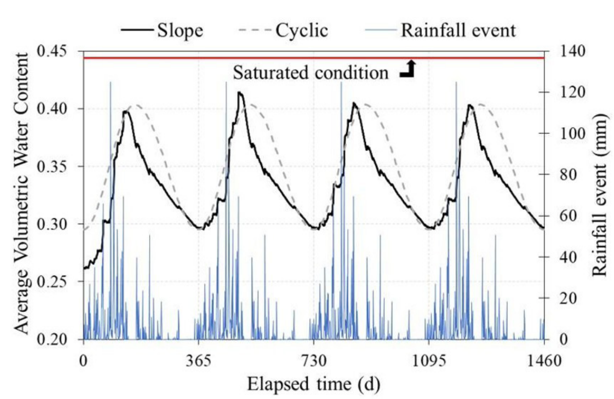

Figure 14. Average volumetric content over time for simulating a habitual climatic year.

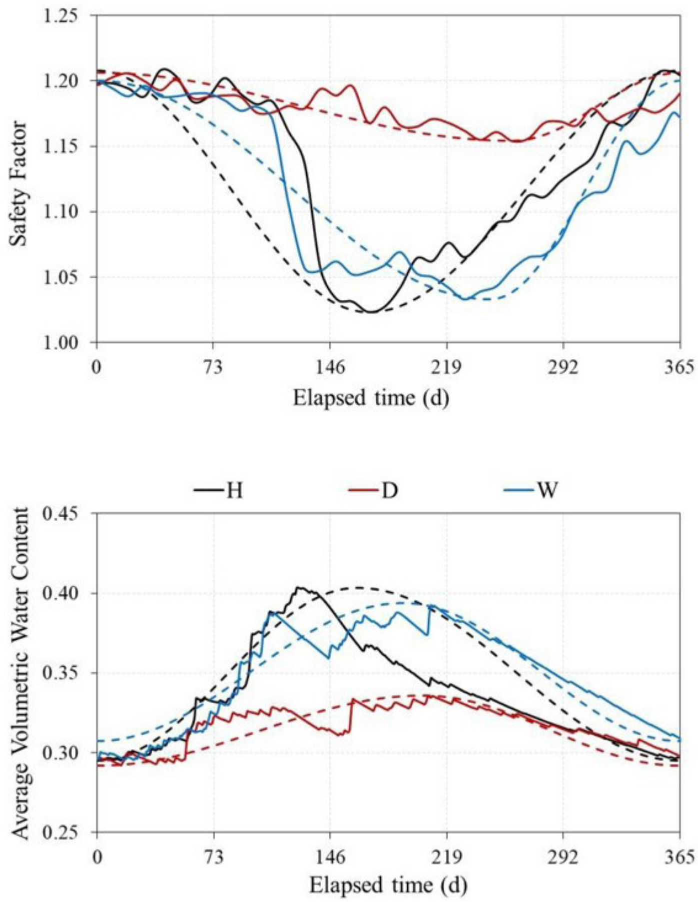

Figure 15. Upper part: variation of the average volumetric water content; lower part: variation of the safety factor with time for habitual (H), dry (D) and wet (W) climatic years.

can be attributed to the high potential for evapotranspiration in tropical regions, mainly due to high temperatures. On the other hand, humid and habitual climate years exhibited similar behavior, despite the significant difference in total precipitation volume. This similarity can be attributed to the complexity of the climatic variables, which exhibit their own gradations and characteristics, thereby influencing the hydrological response of the slope. Nonetheless, these results reinforce the importance of considering the interaction of climatic conditions on slope stability, especially in climate change scenarios, for a more robust and accurate assessment.

4.2.2 Drying effects on shear strength

As discussed in item 2.2, soil drying may affect hydrological soil characteristics due to the formation of cracks, and this must be accounted for in any flow analysis comprising slope stability analyses. However, the potential effects of drying on the shear strength of soils are little discussed, particularly when cracks formation due to drying is not noticed, as commonly found in unsaturated slopes in Rio de Janeiro. Aiming to contribute to that, results of laboratory investigations performed on statically compacted specimens of highly weathered soil (colluvium or mature residual soil) originating from granitic-gneiss rocks from Rio de Janeiro are considered herein.

Figure 16 summarizes the basic properties of the studied soil. As indicated, the soil is clayey; however, due to the mineralogy of its fine fraction (essentially kaolinitic), it comprises a low-activity material that did not crack under drying, as observed by Beneveli (2002) when defining the soil water retention curve (SWRC) of the compacted material.

Following a methodology that has long been used at PUC-Rio in the evaluation of failure mechanisms associated with Rio de Janeiro´s soil slopes (e.g., Moncada et al., 2011; de Campos et al., 2018), the SWRC shown in Figure 16 was obtained, using the filter paper technique, by moistening and drying specimens initially at the w_{ot}. Thus, neither the dried nor the wetted compacted specimens had been previously subjected to the imposed humidity changes and associated suction. Based on this curve, and to further guarantee homogeneity and repeatability of initial testing conditions, it was defined a suction of 63,0 kPa to be initially set to all specimens compacted at the optimum moisture content

G_S	Grain Size			Atterberg Limits (%)		Ac
	Sand	Silt	Clay	w_L	w_P	
2.76	33	9	58	56	31	0.4
Compaction (Proctor Normal)						
w_{ot}				γ_{dmax}		
26.2				14.95		

(a)

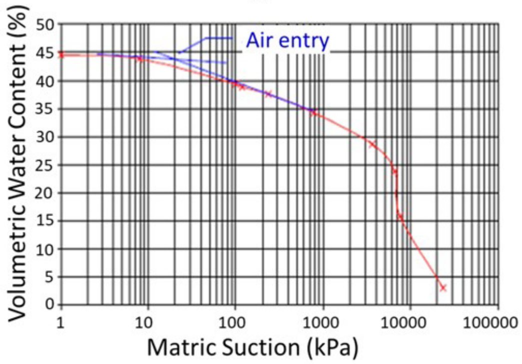

(b)

Figure 16. (a) basic geotechnical properties of the studied soil; (b) SWRC of the compacted soil (Beneveli & De Campos, 2004).

submitted to shear in a PUC-Rio's suction-controlled direct shear test equipment (de Campos & Carrillo, 1995).

To evaluate the effects of drying on the shear strength, direct shear tests were performed on specimens consolidated to an initial suction, u_s, of 63 kPa and net stress of 50 kPa. Subsequently, they were saturated. As shown in Figure 17, one specimen was sheared just after the initial saturation. Other specimens were dried after the initial saturation to suctions of 63 kPa, 120 kPa and 240 kPa. Then, they were saturated again and sheared under a constant rate of displacement.

The results shown in Figure 17 indicate that wetting-drying cycles may promote a not negligible decrease in the drained shear strength of soils, with such a decrease being more relevant the higher the drying introduced within two wetting processes. Comparing the specimens sheared after drying to 63 kPa with those sheared after drying to 120 kPa and 240 kPa, decreases in ultimate strength were of circa 9.5% and 14%, respectively.

5. Further potential atmospheric effects on mass movements

Apart from the recognized effects of climate wetting and drying cycles in the development of gravitational soil-mass movements, the effects of a further atmospheric event – lightning, in this case – cannot be disregarded, as put forward by de Campos et al. (2018). To do so, these authors took as a basis the catastrophic thunderstorm events that occurred in the highland region (Região Serrana) of the state of Rio de Janeiro in 2011, considered by ONU as the 8th major landslide-related disaster occurring in the last 100 years in the world (Busch & Amorim, 2011). In this event, thousands of landslides, with differing slope failure typologies (Amaral et al., 2013; Fernandes et al., 2013), occurred within a few hours of difference on January 11th (night) and 12th (dawn), 2011. The relatively short period of generalized setup of failures did not align with investigations of failure mechanisms typically associated with rainwater infiltration in the involved granitic-gneissic unsaturated soil profile slopes (de Campos et al., 2018). In addition, although the rainfall event was exceptional, it could not be considered unprecedented (e.g., Avelar et al., 2011; Coelho Netto et al., 2011; Medeiros & De Barros, 2011). Additionally, Entralgo (2013) presented evidence that the locus of the highest rainfall intensity did not fully coincide with the location of the scars from the main landslides at the site as a whole. Furthermore, local inhabitants reported the occurrence of continuous lighting and strong vibrations during the storms, indicating the need to investigate whether atmospheric effects related to the occurrence of flashes of lightning and associated thunder sound waves could have contributed to this particular event.

Corroborating this, it is worth noting that Brazil, although not presenting the most world-relevant lightning hotspots (Albrecht et al., 2016), is, due to its tropical nature and continental dimensions, considered the world champion in lightning incidence (Ciência é Tudo, 2022). Bearing this in mind, recent studies have addressed the effects of climate change on the incidence of lightning in Brazil. For instance, Santos et al. (2017) projected the incidence of lightning in the state of São Paulo using CMIP5 climate models in RCP4.5 (intermediate emissions) and RCP8.5 (high emissions) scenarios. A predominance of above-average events is projected for the future, especially in the RCP8.5 scenario, with 93.3% of projected future events expected to be above average. Pinto Junior & Pinto (2020) investigated the relationship between the increase in global temperature and the incidence of thunderstorms in Rio de Janeiro over a 160-year period (1850–2010). The results indicate a 21% increase in the average annual number of days with thunderstorms during the analyzed period, accompanied by a 0.6°C rise in surface temperature. It is also interesting to note that, based on data from ELAT/INPE (Atmospheric Electricity Group at the National Institute for Space Research), ranging from 2005 to 2010, Carnavale (2013) verified an average increase of 40% in lightning incidence in the region affected by the 2011 catastrophe.

5.1 Potential lightning effects on soils

Electric currents generated by lightning are enormous, ranging from approximately 10 kA to 300 kA, with electric voltages varying from 500 kW to 5,000 kW (e.g., Wakasa et al.,

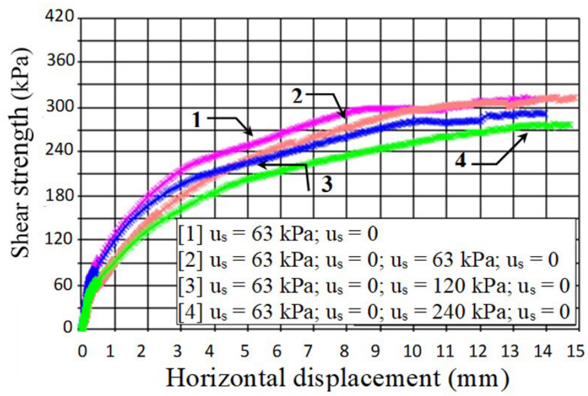

Figure 17. Effects of wetting-drying cycles on shear strength (adapted from Beneveli & De Campos, 2004).

2012). This results in ground temperatures reaching up to 30,000°C (e.g., Newman et al., 1967; Nakano, 1996). As pointed out by Wakasa et al. (2012), due to the hazardous and impulsive nature of lightning and its extremely localized effects, there is limited information in the current literature regarding the ground's response to lightning strikes.

Reviewing pieces of evidence on the direct lighting flash effects on the ground, Wakasa et al. (2012) mention authors who suggest that lighting flashes may trigger changes in the landscape, such as the physical disintegration of rocks, the formation of tors, and the development of gnammas and fractures in the site bedrock. Probably due to the high temperatures involved, it is also known that lighting may promote changes in soil mineralogy (e.g., Mahaney & Milner, 2011). Indeed, the presence of fulgurite minerals in soils and rocks may be related to the effects of lightning strikes (e.g., Rakov, 1999; Elmi et al., 2017). Further lightning shock wave effects on soils, including temperature and osmotic suction ones, have been reviewed by Honke & Karch (2022) and Rao et al. (2022), among others. Evidence also shows that lightning affects soil bacterial communities (Chen et al., 2022).

Due to the difficulties in studying natural lightning strike events on earthen materials, artificial lightning can be generated in the laboratory in research works. Examples of this are provided by Wakasa et al. (2012) for rock specimens and by Carnavale et al. (2016) for soil specimens. These late authors evaluated the effects of simulated laboratory lightning flashes on the shear strength of undisturbed soil specimens from the highland region of Rio de Janeiro affected by the 2011 catastrophe (Figures 18 and 19). Such specimens were confined within thick wall PVC samplers and submitted to simulated lightning strikes under controlled voltages of 300 kV, 450 kV and 600 kV. The basic properties of the tested material are included in Figure 18.

As shown in Figure 19a, the higher the applied voltage of the simulated lightning, the lower the unconfined strength of the soil specimens. Figure 19b shows that, as expected, increasing shear strength occurs under increased initial suction. However, specimens submitted to simulated lightning strikes

Grain size distribution (%)				Average physical properties		
Gravel	Sand	Silt	Clay	G_s	e	ρ_d
1.4	60.5	31.9	6.2	2.66	0.72	1.49

(a)

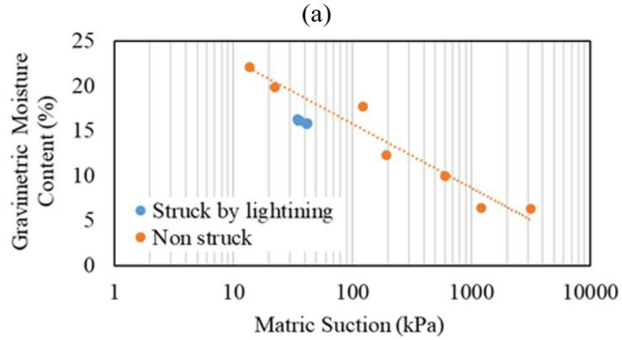

(b)

Figure 18. (a) basic characterization data of the soil tested; (b) partial SWRC of the soil (produced after Carnavale et al., 2016).

showed unconfined strengths much lower than those not struck by lightning, with a decrease in strength ranging from some 50% to 60% as a function of the initial suction of the specimen. Furthermore, as the voltage applied in the laboratory lightning simulations did not encompass the full range of those observed in nature (which may reach up to 5,000 kW), it can be expected that the shear strength of a soil portion directly impacted by a lightning flash will be nearly null.

Regarding soil slope instability processes, it is considered here that the effects of lightning strikes directly onto the ground, although still requiring further investigations, may not be relevant as they are strongly localized. On the other hand, potential processes related to the propagation of seismic waves in the soil resulting from lightning shock waves on a given spot require further investigation. Field monitoring of micro seismic waves propagated by lightning strikes

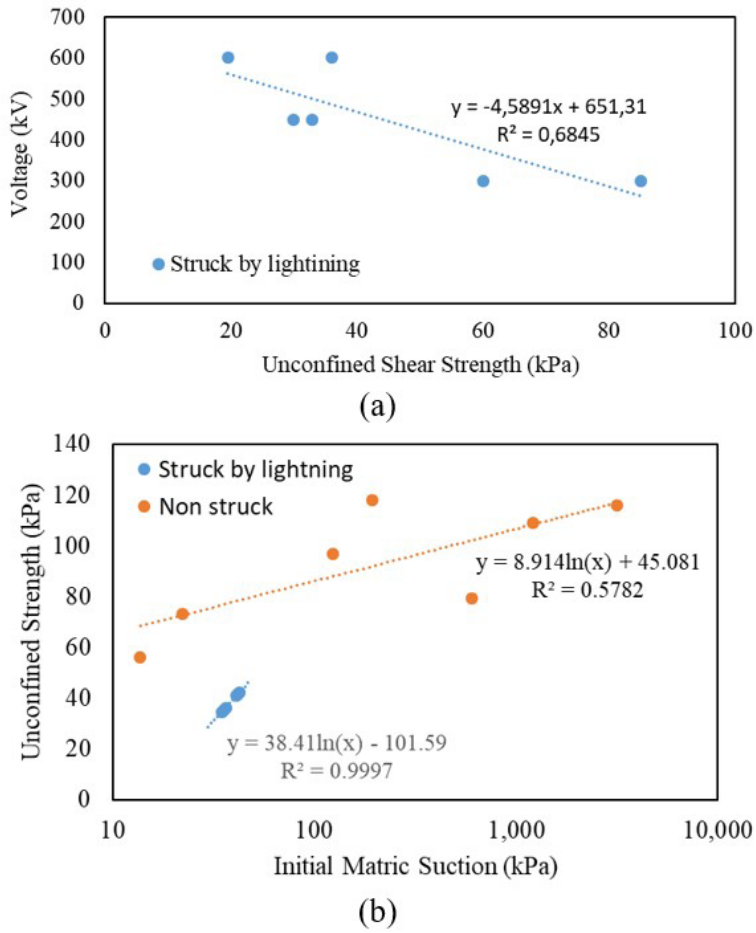

Figure 19. (a) unconfined shear strength variation with the applied voltage; (b) variation of unconfined shear strength with initial suction (adapted from Carnavale et al., 2016).

far from their onset points, reported by Carnavale (2018), supports this view.

5.2 Thunder effects

Acoustic waves transmit the sound of thunder, which cannot be dissociated from the phenomenon of lightning flashes because the heated channels and their pressure signatures are strongly connected (Ribner & Roy, 1984). On the other hand, the thunder's influence area is higher than that of the flashes. Thunder can be heard up to 25 km away, suffering damping or attenuation depending on the geometry of its propagation site (Bass, 1980).

Thunder is a phenomenon that can be explored using the air pressure approach. When dissipated on the earth's surface, thunder can result in a considerable increase in atmospheric pressure. According to data reported in the literature (e.g., Newman et al., 1967), this increase can reach up to 2 atm on the soil. Rakov & Uman (2003) reported a rise of 0.3 atm to 2 atm at a distance of 10 cm to 35 cm from the luminous channel.

Increases in air pressure in the soil have only been observed in cases of advance of the saturation front in the vadose zone. This phenomenon, known as the Lisse Effect, has long been recognized. In this regard, Waswa et al. (2011) include several references from laboratory studies, field observations, and theoretical analyses dating back to the 1930s. As the saturation front advances, the air in the soil's unsaturated zone becomes trapped and compressed, thereby increasing the air pressure in the voids (Waswa et al., 2011; Sakaki et al., 2011). However, as far as the authors are concerned, phenomena related to the effect of thunder-sound waves on the ground have not yet been considered in relation to slope stability, particularly in tropical environments.

In this context, Motta (2016) investigated the effects of a sudden increase in air pressure on the stress-strain-strength behavior of unsaturated soils from natural slopes in Rio de Janeiro. Partial findings of experiments performed on a mature soil from the *Região Serrana* of Rio de Janeiro are reported herein.

The studied soil consists of high-plasticity silt (MH), characterized by a plasticity index of 29% and an activity index of 0.71. The fine fraction is primarily composed of quartz, kaolinite, and gibbsite. Quartz dominates the coarser fraction, including clayey-ferruginous aggregates and traces of magnetite, feldspars, and altered biotite.

The incremental pore size distribution obtained by mercury porosimetry intrusion (MIP) indicates a dual porosity structure of the material. This is reflected in the soil-water retention curve, which indicates a macropores-associated air entry value of approximately 10 kPa and a micropore-related air entry value of more than 1,000 kPa.

Tests were conducted on a double-walled stress-path triaxial apparatus, utilizing the axis translation technique to apply suction to the soil specimens and measuring the total volume change of the unsaturated specimen, as reported by de Campos et al. (2021a). Constant water content (CW) triaxial tests, named CW-x-y, in which x is the initial net confining stress and y is the initial applied matric suction (u_a - u_w), were divided into three series. The first series involved applying different suction levels (20 kPa and 100 kPa) and net normal stresses (40 kPa and 250 kPa) to verify the influence of initial suction on shear strength at both low and high-stress levels.

Series II and III sought to study the effect of a sudden increase in air pressure to the lowest and the highest net normal stress tested at both suction levels. These tests, designated as CWx-y-iz, refer to a sudden increase in air pressure (of the order of 10 seconds' application) imposed on the specimens after consolidation and before shearing. Following Newman et al. (1967), air pressure increments of 20 kPa and 200 kPa were applied to simulate air pressure increases due to lightning under rainstorm conditions.

Results of the CW tests, with and without a sudden increase in air pressure, are shown in Figure 20, comprising plots of deviatoric stress (σ_d) x axial strain (ε_a) and suction ($u_a - u_w$) x axial strain. In these tests, suction was defined by measuring pore-water pressure at the specimen's base. As the air pressure remained constant under shearing, an increase in pore-water pressure implies a decrease in suction.

The stress-strain curves shown in Figure 20 indicate that both stiffness and shear strength decrease due to the applied peaks of air pressure. As indicated by the (u_a-u_w) versus ε_a plots, such decreases are associated with suction decreases under shearing.

These results suggest that atmospheric pressure generated by sound waves resulting from lightning strikes may induce changes in the soil, potentially contributing to the development of failure processes in tropical soil slopes during thunderstorm events.

Further evidence of that has been provided by Carnavale et al. (2014). These authors present results of variations in matric suction during simulated thunder sound wave incidence in confined and unconfined undisturbed soil blocks retrieved from the *Região Serrana* of Rio de Janeiro affected by the 2011 catastrophe. The blocks were installed within a chamber with thermo-acoustic treatment, and six thunder sound wave signal emissions were triggered through computer-controlled high-resolution loudspeakers (Carnavale, 2013), crosschecking the sound pressures with the installed block instrumentation, comprising Trime Pico 32 TDR moisture content (IMKO, 2009), T5X suction probe (UMS, 2009) and delta shear accelerometer (Serridge & Licht, 1987) devices, refer to Carnavale (2013) for details (Figure 21).

These experiments yielded minor variations in suction, ranging from 0.0 kPa to 0.4 kPa. However, they induced the collapse (failure) of three unconfined soil blocks (Carnavale, 2013), suggesting the need for further investigations on this subject.

6. Municipal solid waste landfills and biogas production and emissions

Sanitary landfills remain the predominant method for treating and final disposal of urban or municipal solid waste (MSW) due to their effectiveness, scalability, and lower implementation and operational costs per tonne received. In 2022, according to ABREMA (2023), these facilities treated 61% of the 71,729,841 tonnes of MSW adequately collected in Brazilian municipalities. The remaining 39% were directed to controlled landfills or dumps, which pose various social, environmental, and engineering challenges. Consequently, sanitary landfills are anticipated to address the inadequately managed MSW increasingly.

Once licensed and operational, these facilities are expected to generate positive socio-environmental impacts for the serviced municipalities and financial returns for the owners or concessionaires. As an example, there are three primary remuneration models in Brazil:

i. Based on the mass of waste received, with the service provider compensated by the generator according to the quantity treated, incinerated, and/or landfilled,
ii. Through by-products derived from waste recycling, typically commercialized to local industries as production raw materials or energy inputs,
iii. Via the biogas captured from the decomposition of organic waste, which can generate revenue from carbon credits sold in voluntary or regulated markets, electricity produced from methane and commercialized in distributed generation, and/or gas energy from biomethane, which can be marketed as compressed natural gas or liquefied gas.

The primary technical-scientific challenges comprising revenue from MSW disposal in landfills involve enhancing the efficiency and quality of biogas generation. Efficiency

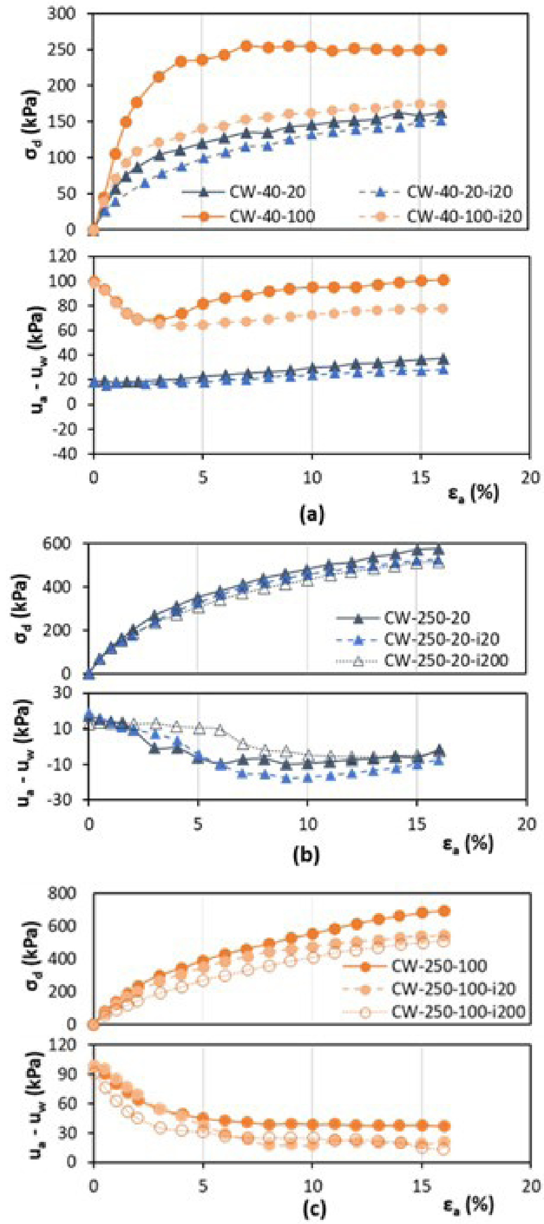

Figure 20. Stress-strain behavior of the mature soil with and without peaks of air pressure increase - (a) under lower net stress (40 kPa), initial suction of 20 kPa and 100 kPa; (b) under higher net stress (250 kPa), initial suction of 20 kPa; (c) under higher net stress (250 kPa), initial suction of 100 kPa.

pertains to capturing the biogas molecule without losses through the collection system or the waste mass. This is achieved by minimizing gas condensation due to pressure and temperature differentials between the landfill's interior and the external environment, preventing oxygen ingress into the collection system and waste mass, and avoiding fugitive methane emissions through the cover material. Quality refers to the biogas composition, which must contain at least 47% methane to ensure the technical and economic viability of the adopted extraction technology.

6.1 Biogas generation and environmental aspects

Several factors can influence biogas generation in sanitary landfills, including:

i. Local topography and geometric configuration of the landfill, as waste masses on slopes or in mining pits, reduce their exposed surfaces, limiting oxygen access and methane emissions,
ii. Waste typology, with landfills receiving more organic matter having higher methane generation potential,

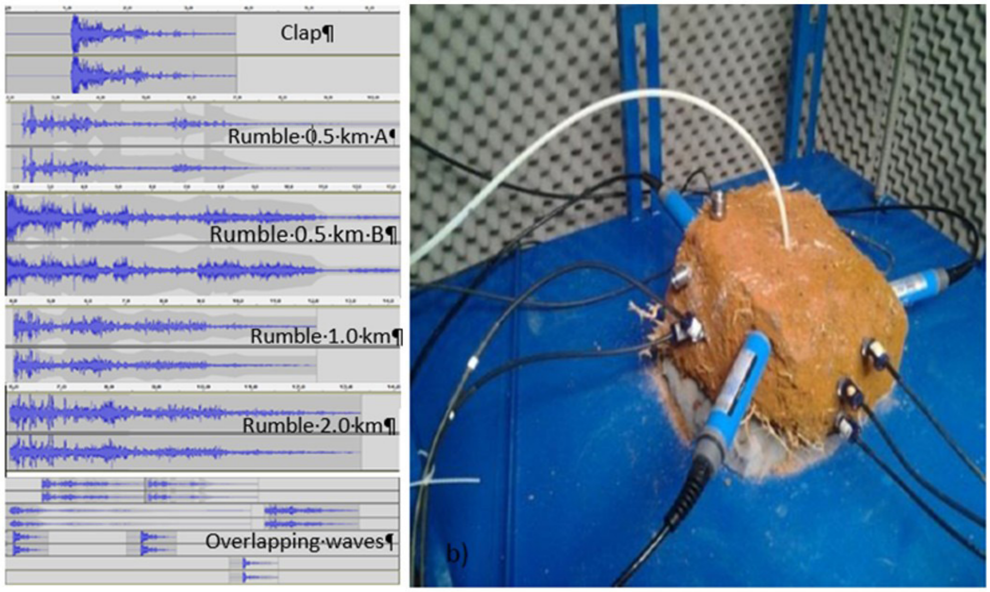

(a) (b)

Figure 21. (a) replicated thunder sound wave signals (Lee, 2009); (b) typical instrumented sample setup (reproduced from Carnavale, 2013).

iii. Waste characteristics, which vary over time in terms of temperature, humidity, and organic matter concentration, potentially inhibiting anaerobic biodegradation,
iv. Cover material properties, such as air permeability, density, humidity, and layer thickness, which can affect hydraulic and pressure gradients with the external environment,
v. Presence of synthetic covers, like high-density polyethylene (HDPE) or low-density polyethylene (LDPE) geomembranes, which further restrict contact between the waste mass and the external environment,
vi. Internal biogas pressure gradient relative to atmospheric pressure,
vii. Distance and efficiency of vertical drains in forced or natural gas extraction,
viii. Biogas capture and utilization technologies, which may follow different technological routes,
ix. Location, climate, and seasonality, as external environmental conditions can impact cover material properties, structural behaviour of the waste mass, degradation rates, and microbial activity.

To gain a first view of the interaction of some of these factors, historical data was collected from sanitary landfills and their biogas generation across two regions of Brazil – southeast and northeast – and they were analysed considering environmental aspects (Figures 22 and 23).

Initially, the data shows that biogas generation is directly proportional to the size of the landfill. Larger units generate more biogas in absolute terms because they have more stored MSW (Figure 22a). However, when normalizing the generation based on the daily intake rate of each site (Figure 22b), the results show that the largest generators are not the most efficient, meaning those that produce more biogas per tonne of waste received. This confirms that other factors influence landfill biogas generation.

As indicated in Figure 23, some trends are observed when evaluating environmental variables, such as rainfall, temperature, and atmospheric pressure (represented, in this case, by the landfill elevation), at each location. In this figure, the average monthly biogas production was normalized by the waste daily intake rate, as mentioned before.

As shown in Figures 23a to 23c, less rainy regions tend to provide more efficient biogas generation, even on an annual average, during the dry or rainy seasons. Since the natural cover layer is composed of unsaturated soil, predominantly consisting of fines, typically silts and clays, it has lower thermal conductivity, thus reducing heat and moisture exchanges between the interior of the waste mass and the external environment.

Regions with higher average temperatures tend to exhibit more efficient biogas generation, as illustrated in Figures 23d and 23e, during both the dry and rainy seasons. Environments with higher temperatures tend to reduce heat exchanges with the waste mass's interior, reducing the volume of fugitive emissions through the cover system. Thus, more efficient generation may be achieved.

Regions subject to higher atmospheric pressures (lower elevations) provide more efficient biogas generation, as presented in Figure 23f. Higher external atmospheric pressure will reduce the pressure gradients through the landfill cover system, thus reducing fugitive emissions and enabling more efficient biogas production.

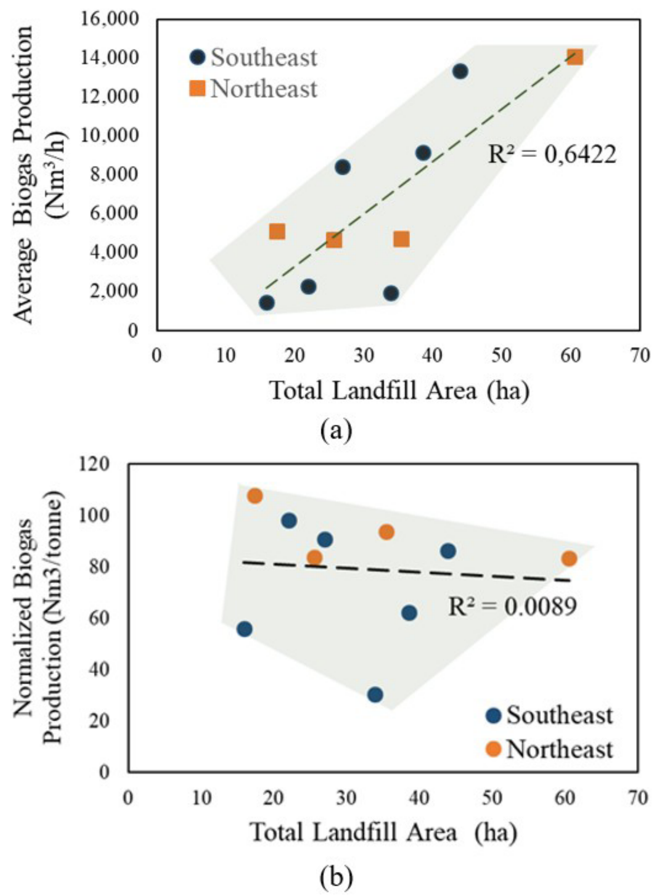

Figure 22. (a) relationship between the maximum biogas production and the total landfill area; (b) relationship between the normalized biogas production and the total landfill area.

6.2 Biogas emissions: general aspects

Climate change and the need to reduce greenhouse gases (GHGs), including methane, have driven global initiatives under the United Nations Framework Convention on Climate Change (UNFCC), as well as the United Nations Environment Programme (UNEP, 2024). COP 29, held in Azerbaijan in November 2024, drafted the Declaration on Reduction of Methane from Organic Waste. This document focuses on adopting practices such as composting, recycling organic waste, and capturing gas in landfills for energy generation. These solutions have already been implemented in some countries and have shown efficiency in reducing emissions and reusing waste as economic resources.

The United States is the second-largest emitter of GHGs, and landfill disposal is the third-largest source of emissions. According to the EPA (United States, 2018), the country has reduced landfill emissions by up to 40% with the adoption of control systems and an increase in biogas capture. In the European Union (EU), countries with efficient MSW management systems generally perform better in global waste management. According to Eurostat (Statistical Office of the European Union) data from 2018, the waste sector's emissions reduction was 29.7%. Latin America's solid waste management system is primarily focused on the final disposal of waste in landfills, accounting for approximately 60% of emissions from the waste sector in the 10 Latin American countries considered.

Brazil is the fifth largest emitter of methane in the world. Alone, it emits the equivalent of 5.5% of the planet's methane. The waste sector represents the third-largest emitter of GHGs, with around 92 million tons of CO_2eq, or 15.8% of total Brazilian emissions. In the urban solid waste sector, landfills and dumps are responsible for 61.8% of GHG emissions (ABREMA, 2023). This results from Brazil's practice of sending 95% of its waste to landfills rather than seeking sustainable technological alternatives to treat the 80 million tons of waste generated annually. The International Solid Waste Association (ISWA) pointed out that landfills located in Brazil emitted an average of 20 kg of CH4 per tonne of waste disposed of in landfills (Scharff, 2021). This corresponds to a percentage of emissions or losses to the atmosphere ranging from 30% to 38% of the gases generated at the landfill, depending on operational aspects, local climate, anaerobic versus aerobic

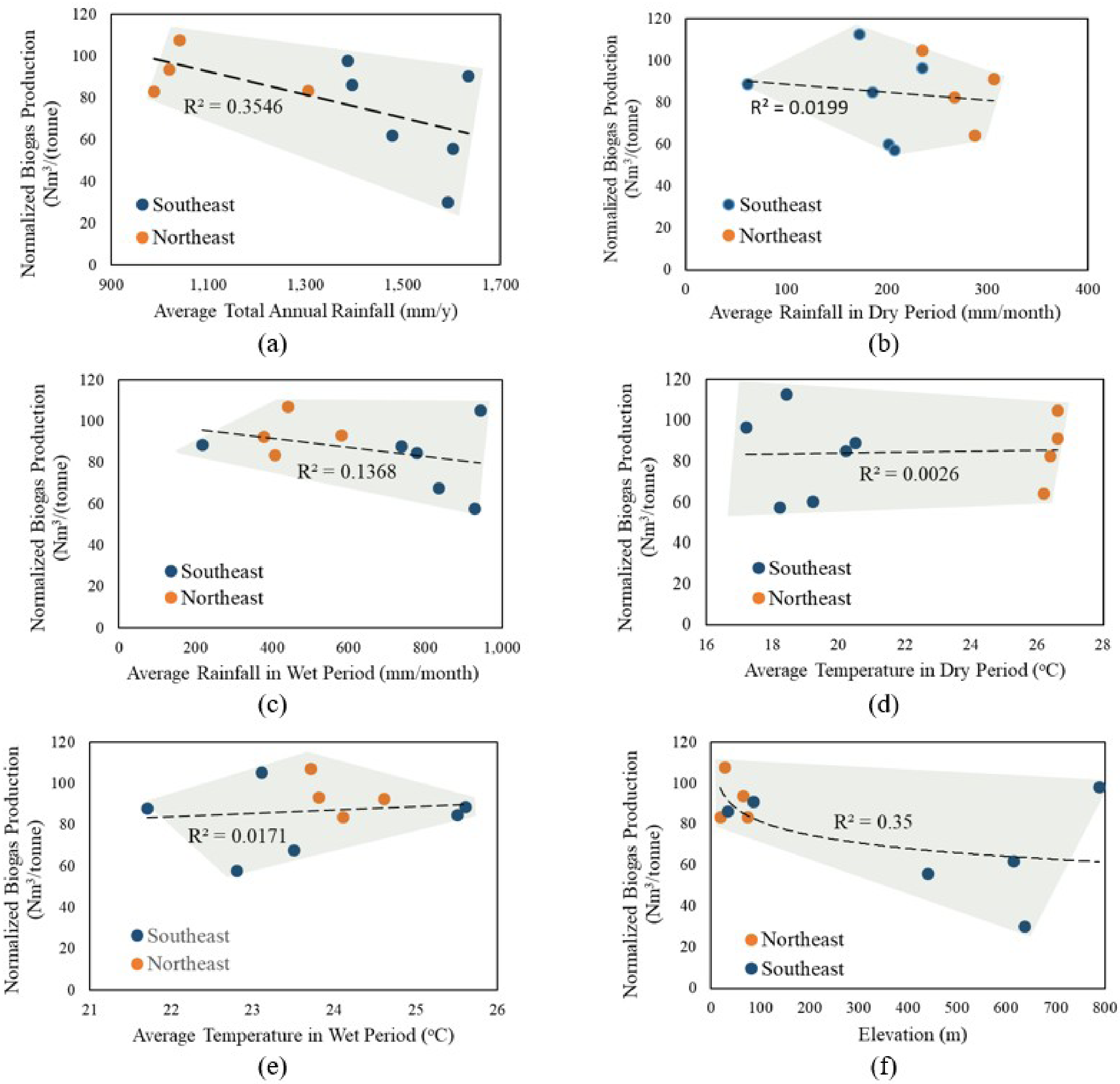

Figure 23. Some relationships between climate variables and normalized biogas production.

conditions, the degradable organic fraction, and whether biogas is captured for energy use. These numbers are estimates based on models from the IPCC (Intergovernmental Panel on Climate Change), which, for many, is considered conservative regarding the actual quantification of emissions in the sector.

6.3 Methane emissions in Brazil

Methane emissions vary greatly depending on various geotechnical factors of the cover layer and the environmental aspects of the landfill location. Among the main aspects that can interfere with gas emissions from the landfill cover layer are variations in soil characteristics, such as soil type, degree of compaction, saturation, and cover layer thickness; variations in waste characteristics, such as internal pressure in the gas mass and in the external contact-soil-atmosphere, which is strongly influenced by the age of the waste (e.g., Schirmer et al., 2014), and climatic conditions.

As for atmospheric factors, all aspects of the climate are fundamental, as they affect the humidity of the layer, increasing its saturation and reducing its air permeability and emissions in rainy periods. Depending on the internal pressure of the biogas in the landfill (which is usually very small due to the presence of the installed gas drainage system), atmospheric pressure, despite having little influence, can significantly alter the pressure gradient between the internal and external environments. For instance, a gradient inversion causes air ($N_2 + O_2$) to enter the landfill at certain periods, resulting in a significant change in the gas composition in the surface layers of the landfill. Another relevant aspect of the climate is the increased infiltration in landfills, which increases the level of leachate in the waste mass and reduces emissions. Furthermore, waste requires a humid environment for facultative microorganisms to perform their function, degrading the waste and generating biogas. However, when the waste is saturated, biogas is not generated. Lastly, but also importantly, the climatic conditions associated with the soil characteristics in the cover layer can cause cracks in the layer, which significantly increase emissions. During the dry season, when the soil in the cover layer has lower humidity and larger suction, a very favorable environment for emissions is created due to the high air permeability of the soil in the cover layer and the preferential paths of crack's water flow generated by soil contraction.

To quantify CH_4 superficial flux on the landfill cover layer, it was used the static flux chamber technique (Mariano & Jucá, 2010; Maciel & Jucá, 2011; Almeida et al., 2024). Further methodologies, such as robotic systems for mobile detection of emissions (e.g., Bennetts et al., 2012), UAV-based thermal imaging, or advanced monitoring systems using remote sensing from aircraft (including drones), and satellite sensors, may also be employed (e.g., Henn & Peduzzi, 2024). However, besides limitations on the amplitude of the investigation area (the best is of the order of 30 m), they do not provide information on the geotechnical characteristics of the cover soil, which must be obtained via field and laboratory geotechnical investigations anyway (e.g., Belfort et al., 2018). In this sense, the static flux chamber technique is mandatory (see Figure 24), either as a unique or complementary one. Its only disadvantage is that several points from a given landfill area must be evaluated.

In what follows, the data presented focuses on quantifying full-scale methane emissions from Brazilian landfills, aiming to establish a simple methodology that can be applied to any landfill type. This quantification can guide public and private managers on the best techniques to identify, quantify, and reduce landfill emissions.

The reported landfills, of different sizes, are from the Northeast, Center-West, and Southeast regions of Brazil. The methodology used to evaluate the gas emission through the top covers consisted of CH_4 superficial flux quantification using the static flux chamber and evaluating biogas and soil parameters in depth until the contact with the solid waste.

Various parameters can be measured, like CH4, CO2, and O2 concentration, internal temperature (between the chamber and the top cover), external temperature, and internal and atmospheric pressures. Several tests are carried out for soil characterization, such as grain size distribution and Atterberg limits, Proctor compaction curve, water permeability, and soil-water characteristic curve. Typically, the testing duration varies from 30 minutes to 60 minutes, and the initial slope of the plot of the CH_4 mass-versus-time determines the gas flux. The following equations (Equations 4 and 5) are used to determine the volumetric and mass CH_4 flux rates:

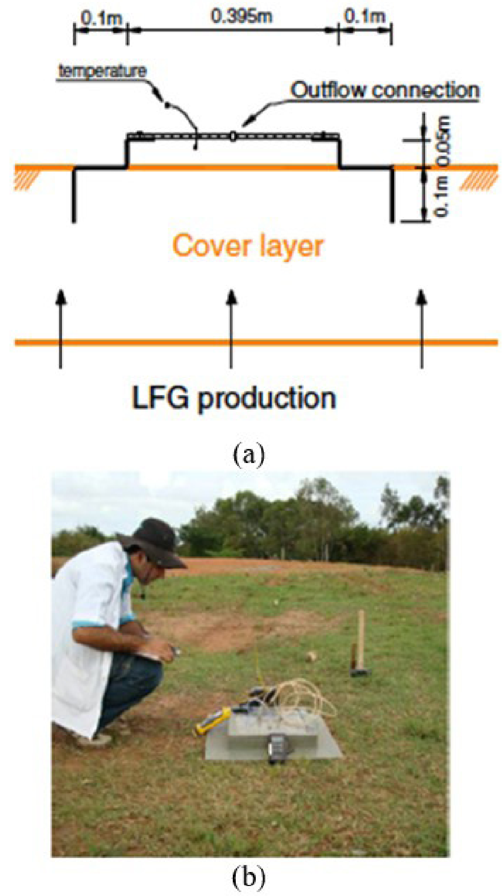

Figure 24. Measurement of fluxes of CH_4 using the static flux chamber technique - (a) layout - LFG = landfill fugitive gas; (b) field monitoring.

$$Q_{CH_4} = \frac{V}{A} x \frac{\Delta C_{CH_4}}{\Delta t} x \frac{273.15}{273.15 + T} x \frac{P_{atm}}{1{,}000} \quad (4)$$

$$J_{CH_4} = Q_{CH_4} x \rho_{CH_4} \quad (5)$$

where:

Q_{CH4} is the volumetric superficial flux rate of CH_4 (NL/s m^2), J_{CH4} is the mass superficial flux rate of CH_4 (g/s m^2), V is the internal chamber volume (of 8.34 L), A is the cover soil area (of 0.156 m^2), $\Delta C_{CH4} / \Delta t$ is the CH_4 concentration increase (% vol.) with time (s), T is the gas temperature inside the chamber (^{o}C), P_{atm} is the atmospheric pressure (mbar), and ρ_{CH4} is the specific mass of CH_4 (g/L).

Table 2 presents emissions data from 14 Brazilian landfills located in different regions and states. It shows the amount of MSW entering per day, the landfill area at the time the studies

Table 2. Measurements of methane emissions in some Brazilian landfills.

Landfill	MSW (tonne/day)	Max flow CH_4 (g/m^2.day)	Landfill area (m^2)	ISWA (kg CH_4/tonne waste)	Characteristics of the cover layer (Thickness; soil classification; Sr; DC; Specific Weight; Cracks)
Northeast (CE)	5	311.0	733,6	46	0.8m; ML; Sr = 75%; CD = 85%; 19 kN/m^3; no
Northeast (PB1)	450	123.7	300	82	0.6m; MH; Sr = 58%; CD = 99%; 19 kN/m^3; no
Northeast (PB2)	900	331.3	90	33	1.1m; MH; Sr = 42%; CD = 98%; 17 kN/m^3; no
Northeast (RN1)	1,3	202.3	450	70	1.0m; SC; Sr = 50%; CD = 90%; 16.9 kN/m^3; no
Northeast (RN2)	1,2	240.4	352,7	71	0.67m; ML; CD = 93%; 16.8 kN/m^3; no
Northeast (PE1)	2	362.9	600	109	0.8m; CL; Sr = 75%; CD = 85%; 19 kN/m^3; no
Northeast (PE2)	450	400.0	20	18	0.4m; SC; Sr = 55%; CD = 95%; 18 kN/m^3; yes
Northeast (PI)	700	351.4	340	171	0.8m; CL; Sr = 75%; CD = 85%; 19 kN/m^3; no
Center-West (DF)	2,64	123.3	110	5	1.4m; CH; Sr = 80%; CD = 88%; 18 kN/m^3; no
Southeast (MG)	3,8	337.7	143,953	13	0.34m; MH; Sr = 45%; CD =9 1%; 16 kN/m^3; yes
Southeast (RJ)	10	389.1	1,005,331	39	0.8m; CH; Sr = 75%; CD = 85%; 19 kN/m^3; yes
Southeast (SP1)	5,5	300.0	202,341	11	0.67m; CL and ML; CD = 93%; 16.8 kN/m^3; no
Southeast (SP2)	6,5	675.0	760	79	0.55 to 1.0m; CL and ML; CD = 90%; 16.5 kN/m^3; no
Southeast (SP3)	2,983	277.8	323,863	30	0.6 to 0.9m; ML and CL; CD = 97%; 18.5 kN/m^3; no

CE = Ceará; PB = Paraíba; RN = Rio Grande do Norte; PE = Pernambuco; PI = Piauí; DF = Federal District; MG = Minas Gerais; RJ = Rio de Janeiro; SP = São Paulo; Sr = degree of saturation at compaction; CD = compaction degree in relation to Normal Proctor.

were carried out, the maximum flow of methane (in g/m^2.day), the rate of methane emissions per ton of waste entering the landfill (Scharff, 2021), and the characteristics of the cover layer.

As can be seen, methane emissions values are, in most measured cases, higher than those recommended by ISWA, which would be up to 20 kg CH_4/tonne of waste (Scharff, 2021). These data can be even more alarming if presented regarding total CH_4 emitted ($MgCO_{2eq}$). It can be concluded that many landfills in Brazil need to evaluate their cover layers better to mitigate methane emissions to the atmosphere. In small and medium municipalities in Brazil, landfill gases are usually thrown into the atmosphere without any treatment, leading to environmental pollution. In addition, Brazilian standards do not emphasize the technical aspects of the final cover layers of landfills. An example that can provide relevant insides on the design of such type of barrier is given next.

6.4 Physical modelling of a sanitary landfill final cover layer

In municipal sanitary landfills, the final cover comprises the boundary directly interacting with the atmospheric environment. An effective cover layer reduces water infiltration (and leachate generation) and fugitive gas emissions. Furthermore, it propitiates a truly anaerobic decomposition environment for waste decomposition. In such structures, due to the clayey nature of cover layers, many cracks appear due to the wetting/

drying climatic cycles and differential settlements of the waste mass, severely impairing the cover layer performance.

Lôbo et al. (2023) present the development of a 2D instrumented channel (see Figure 25) that controls insolation, rainfall, temperature, and air humidity and monitors moisture content, suction, runoff (ROD), and bottom drainage (BLD) to evaluate the performance of cover layers submitted to controlled environmental conditions in the laboratory.

The performance of capillary (CB) and conventional monolithic (CV) barriers was assessed for a period of about one year. The capillary barrier was formed by a clayey layer of a mature residual soil from granulite-gneiss embedment overlying a uniform layer of fine dune sand. The internal monitoring of CB barriers considered the hydraulic differences between the layers. In both soils, temperature, electrical conductivity and moisture content were monitored using 5TETM moisture sensors (Meter Group, USA). Matric suction in the clayey layer was monitored using MPS-6™ (Meter Group, USA) suction sensors, whereas low-capacity tensiometers (LCT, Sousa et al., 2011) were used in the dune sand layer (see Lôbo, 2022 for details).

Lôbo et al. (2023) highlight the importance of the air relative humidity in the experiments: tests performed on arid conditions presented eight large cracks crossing the entire clayey layer in the first fifteen testing days. In contrast, the test performed with higher relative humidity identified only two main cracks during the whole testing period. Comparing capillary and conventional barriers, the infiltration water reached the clayey layer bottom on day 127 in the CB test, and the total leaked water corresponded to 5 mm or about 1.89% of the amount of rain. In contrast, 14.4 mm, corresponding to about 10.7%, was monitored for the monolithic barrier under the same imposed rainfall conditions.

Figure 26 illustrates typical results in terms of water content and suction obtained in the CB layer.

In the upper portion of the clay layer, Figure 26a shows the fast response of the water content sensors to the imposed rainfall conditions. As infiltration demands time, a delay in the response to changes in the water content at 15 cm and 25 cm is observed. In all cases, increased and decreased water content are respectively related to the wet (imposed by rainfall) and dry (imposed by the Philips™ HPI-400 W metal-halide lamp's energy) simulated environmental conditions. Changes in the bottom sand layer moisture content related to rainfall started only after day 248 of the experiment.

The suction changes in the clayey layer shown in Figure 26b also correlated well with the wet and dry simulated conditions, decreasing in the presence of rain. In the sand bottom layer, the fast suction decrease shown in Figure 26b around day 248 of the experiment agrees with the observed large increase in moisture content.

The above-summarized results show that using a physical model such as that developed by Lôbo et al. (2023) provides a valuable alternative to evaluating different cover layouts under controlled climate conditions close to those at the landfill site.

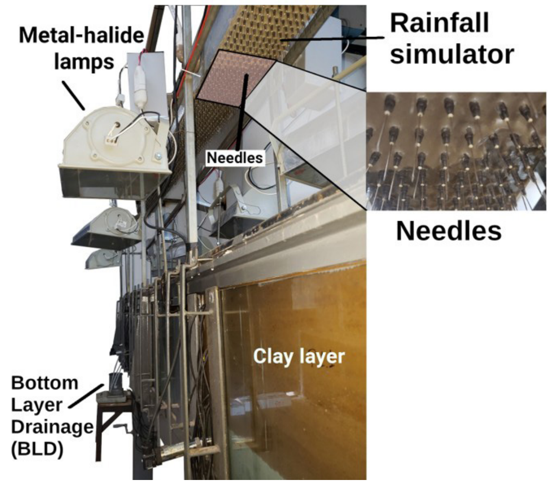

Figure 25. Details of 2D channel developed by Lôbo (2022).

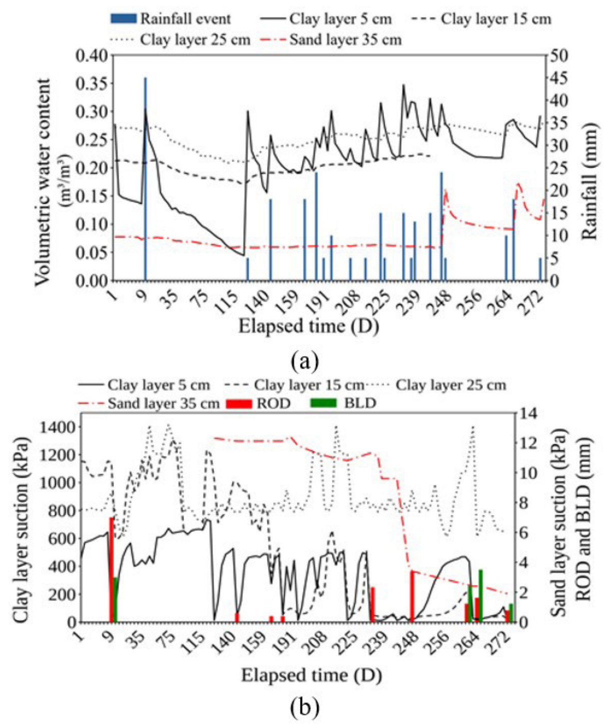

Figure 26. (a) water content and rainfall events in a CB over time; (b) suction measurements, run-off (ROD), and bottom layer discharges (BLD) (Modified from Lôbo et al., 2023).

7. Final remarks

Although soil-atmosphere interactions are relevant to many areas of knowledge and are investigated by scientists of variable technical backgrounds, they are not fully understood due to their complexity, which increases even more if vegetation is included in the processes.

Considering the geotechnical and correlated areas of study, only some aspects comprising soil-atmosphere interactions were herein addressed, all associated with unsaturated soils. The first aspect, related to natural hazards that anthropic actions can enhance, comprises the development of erosion and slope instability processes. The second aspect is related to the final disposal of urban waste in sanitary landfills and its consequences.

Before going further, it is important to note that both aspects considered herein are and will be affected by the so-called climatic changes or, maybe in a better way, the observed global warming. In this sense, heavy and more frequent storms (thunderstorms) and more severe drought periods are to be expected. Recalling the hydric balance equation (Equation1) and Figures 1 and 2, only the *precipitation* variable may be taken numerically as solely dependent on atmospheric changes. The *evaporation* variable, already a difficult one to numerically evaluate, will keep being so in the presence of severe soil drying conditions. Considering the soil compartment, hydromechanical properties are bound to change along the soil profile, with more important changes occurring within the active zone, whose depth may also change under new extreme atmospheric conditions.

Taking into account the above, and based on a comprehensive literature review, as well as the results of research projects developed by the authors, the following final observations are considered herein:

- There are few field observations on the thickness or depth of the active zone in soil profiles, particularly in tropical and semi-tropical areas such as Brazil. This comprises basic information to be pursued as this zone is the one most affected by atmospheric changes. Taking into consideration the limited available information on that, it is desirable to monitor in the field (flat ground) changes over time time (in years) of profiles of the soil temperature and of the volumetric moisture content up to a minimum depth of 5 m;
- In the absence of reliable information on evaporation conditions at a given site, an empirical assessment to be used in numerical flow analysis was introduced. The development of a data bank containing information on evaporation under variable micro-climatic conditions is desirable and must be pursued;
- Desiccation cracks may be formed at the ground surface under drying atmospheric conditions. This affects the hydromechanical behaviour of the soil profile and, thus, must be considered in geotechnical works. Proposals from the current literature on evaluating crack intensity and depth of influence were put forward. However, further research on this topic is required, particularly in the case of tropical soils;
- Erosion setup and development are strongly related to micro-climatic cycles of wetting-drying processes, and this has to be accounted for, particularly in the presence of global warming. The presented case study on erosion clearly shows the relevance of the soil-atmosphere interaction in the different phases of hydric erosion, going from superficial erosion to gullying and its evolution;
- Two aspects of slope stability analysis were emphasized. The first refers to defining the initial moisture content profile along the layers of a soil slope. This basic information, not usually provided by field instrumentation, is relevant for the flow analysis required to define critical suction profiles to be considered in subsequent stability analysis under variable atmospheric conditions. In this aspect, the adoption of representative boundary conditions is fundamental, particularly the basal (or inferior) boundary, which strongly influences the results obtained. The second emphasized aspect was that under extreme (or not experienced before) drying, the soil strength of the non-cracked soil may decrease. Naturally, this may affect the stability analysis's result importantly and, therefore, requires further investigations comprising natural, intact materials that prevail in regions with differing climatic conditions;
- Regarding slope instability processes, the possibility was introduced that lightning originating from thunderstorms may contribute to the onset of landslides. Bearing in mind that flashes of lightning are punctual, it is believed that the main effect to be considered is related to the associated changes in atmospheric pressure that occur and, so, to the resultant change in air pressure within the unsaturated soil. In this case, the results of laboratory simulations on air pulses over unsaturated soil specimens indicated deterioration of both shear strength and stiffness, suggesting that this little-investigated effect may be relevant. A further aspect that requires extensive investigation is the possibility that micro-seismic waves resulting from the effects of lightning flashes may also contribute to the onset of instability mechanisms on the initially unsaturated tropical soil slopes;
- Considering municipal waste disposal in sanitary landfills (MSWL), some results were put forward by crossing data on total biogas production over a given time period and atmospheric data for landfills from different locations in Brazil. These data indicated that biogas production might be affected by the landfill's location and specific site climate conditions, with such production varying with atmospheric-related data such as total annual rainfall, average temperature, wet and dry periods, and atmospheric pressure. Some of these data, however, must be seen with care as they refer to landfills with differing management conditions and strategies for biogas exploitation, aspects that were not considered herein;
- Still regarding MSWL, numbers of biogas emissions from a few Brazilian monitored sites were collected.

However, correlations between such type of data and atmospheric site conditions were possible to derive, either because variations in climatic conditions within the sites were not relevant or, more importantly, differing final soil cover procedures were adopted. In this context, it has to be considered that there is a lack of recommendations (e.g., proposed normalization rules) related to the design of the final cover for MSWL, at least in Brazil. Contributing to that are included results of a physical experimental model that is able to simulate the design of final cover structures, an aspect that requires further investigations;

- Finally, this study reinforces the critical role of soil-atmosphere interactions in geotechnical engineering, particularly in tropical regions liable to extreme climatic events. The results underscore the necessity of incorporating transient modeling techniques to better predict slope stability, erosion, and biogas emissions. Future research should focus on refining numerical models, implementing field monitoring techniques, and assessing long-term climate impacts on geotechnical structures.

Acknowledgements

The authors would like to thank the institutional support in terms of personnel, finances and scholarships that were relevant in enabling the research and training of professionals to work with a focus on sustainable development, providing the basis for the preparation of this article. We want to thank: the National Council for Scientific and Technological Development (CNPq), Coordination for the Improvement of Higher Education Personnel (CAPES), Rio de Janeiro State Research Supporting Foundation (FAPERJ), Goiás State Research Support Foundation (FAPEG), Federal District Research Support Foundation (FAP/DF), Pernambuco Research Support Foundation (FUNAPE), Scientific and Technological Enterprises Foundation (FINATEC), University of Brasília (UnB), Federal University of Goiás (UFG), Federal University of Pernambuco (UFPE), Federal University of Bahia (UFB). Pontifical Catholic University of Rio de Janeiro (PUC-Rio), National Electric Energy Agency (ANEEL), Furnas Centrais Elétricas S.A., Geotechnical Institute for Rehabilitation of the Slope-Plain System (REAGEO/COOPE/UFRJ) and ALTA Geotecnia Ambiental. The authors are also grateful to the reviewers for their useful comments and suggestions.

Declaration of interest

The authors have no conflicts of interest to declare. All co-authors have observed and affirmed the paper's contents, and there is no financial interest to report.

Authors' contributions

Tácio Mauro Pereira de Campos: conceptualization, supervision, project administration, validation, critical review of the manuscript. Mariana Ferreira Benessiuti Motta: investigation, methodology, laboratory tests, writing original draft item 5, critical manuscript review. Nicolas Rodrigues Moura: investigation, methodology, numerical tests, writing original draft item 4, critical manuscript review. Elisangela do Prado Oliveira: investigation, methodology, laboratory tests, writing original draft item 2, critical manuscript review. Álvaro de Freitas Viana: data validation, writing original draft item 6, critical manuscript review. José Camapum de Carvalho: data validation, writing original item 3, critical manuscript review. José Fernando Thomé Jucá: data validation, writing original item 6, critical manuscript review. Sandro Lemos Machado: writing original items 2 and 6, critical manuscript review.

Data availability

The datasets generated and analyzed during the current study are available from the corresponding author upon request.

Declaration of use of generative artificial intelligence

No aspects of artificial intelligence were employed in the technical development of the manuscript. However, the software Grammarly was employed as a tool to help to improve English language use.

List of symbols and abbreviations

2D	Two dimensional
c'	Intrinsic cohesion
e	Void ratio
k_{sat}	Saturated hydraulic conductivity
n	Porosity
w_L	Liquidity limit
w_{ot}	Optimum Proctor moisture content
w_P	Plasticity limit
A	Cover soil area
A_c	Skempton activity index
AE	Air entry value
Be	Basal or lower frontier water flow
BF	Basal frontier
BLD	Bottom drainage
CB	Capillary
CD	Compaction degree in relation to Normal Proctor
CE	Ceará
CH_4	Methane

CMIP5	Coupled Model Intercomparison Project Phase 5
CO_{2eq}	Carbon dioxide equivalent
COP 29	29th meeting of the Conference of the Parties (COP) to the UN Framework Convention on Climate Change (UNFCCC)
CV	Conventional monolithic
CW	Constant water content triaxial tests
CW-x-y	Constant water content triaxial tests, in which x is the initial net confining stress and y is the initial applied matric suction (u_a - u_w)
CWx-y-iz	Constant water content triaxial tests, in which x is the initial net confining stress, y is the initial applied matric suction (u_a - u_w) and iz is the applied air pressure increment
DF	Federal District
DLF	Downstream lateral frontier
E	Evaporation
E	Modulus of elasticity corresponding to the effective normal stress
ELAT/INPE	Atmospheric Electricity Group from the National Institute of Spatial Research
E_p	Potential evaporation
ET	Evapotranspiration
EU	European Union
FEM	Finite Element Method
FF	Free water flow within the soil mass
GHGs	Greenhouse gases
GO	Goiás
G_s	Relative density of grains
H	Modulus of elasticity related to suction
HDPE	High-density polyethylene
I	Infiltration
IPCC	Intergovernmental Panel on Climate Change
ISWA	International Solid Waste Association
J_{CH4}	Mass superficial flux rate of CH_4
K_0	Ratio between the total horizontal and vertical stress before the desiccation process; ratio between the net horizontal and vertical stresses.
LDPE	Low-density polyethylene
MCV	Tropical Compacted Miniature Methodology Tests
MG	Minas Gerais
$MgCO_{2eq}$	Megatonne of carbon dioxide equivalent
MH	High-plasticity silt
MIP	Mercury porosimetry intrusion
MSW	Municipal solid waste
N_2	Nitrogen
O_2	Oxygen
ONU	United Nations
P	Precipitation
P_{atm}	Atmospheric pressure
PB	Paraíba
PE	Pernambuco
PI	Piauí
PUC-Rio	Pontifical Catholic University of Rio de Janeiro
PVC	Polyvinyl chloride
Q	Unity flow
Q_{CH4}	Volumetric superficial flux rate of CH_4
ρ_{XH4}	Specific mass of CH_4
RCP4.5	Representative Concentration Pathway which stabilizes radiative forcing at 4.5 Watts per meter squared
RCP8.5	Representative Concentration Pathway which stabilizes radiative forcing at 8.5 Watts per meter squared
RJ	Rio de Janeiro
RN	Rio Grande do Norte
RO	Runoff
ROD	Runoff
R_{sc}	Soil-Cracking Ratio
SL	Shrinkage limit
SP	São Paulo
SPT	Standard Penetration Test
Sr	Degree of saturation at compaction
$Ss(t-t_0)$	Variation in the soil-water stock (or soil-water volume) over time
SWRC	Soil-water retention
T	Gas temperature inside the chamber
T5X	Pressure Transducer Tensiometer
TDR	Time Domain Reflectometry
TF	Top frontier
TMI	Thornthwaite Moisture Index
u_a - u_w	Matric suction
UAV	Unmanned aerial Vehicle
ULF	Upstream lateral frontier
UNFCC	United Nations Framework Convention on Climate Change
u_s	Initial suction
UWSL	Urban waste disposal in sanitary landfills
V	Internal chamber volume
V_{w0}	Initial water volume
Z_c	Depth of the crack
γ_{dmax}	Maximum dry specific weight
ε_a	Axial strain
θ_m	Volumetric moisture content
μ	Poisson's ratio
ρ_d	Dry density
σ_d	Deviatoric stress
σ_t	Tensile strength of the soil
ΔCCH4 /Δt CH_4	concentration increase with time
$\Delta(u_a-u_w)$	Variation in matrix suction
Y	Total specific weight
ϕ'	Angle of internal friction
ϕ^b	Angle indicating the rate of increase in shear strength with respect to a change in matric suction

References

Abbaszadeh, M.M., Houston, S.L., & Zapata, C.E. (2015). Influence of soil cracking on the soil-water characteristic curve of clay soil. *Soils and Rocks*, 38(1), 49-58. http://doi.org/10.28927/SR.381049.

Adler, R.F., Gu, G., Sapiano, M., Wang, J.J., & Huffman, G.J. (2014). Global precipitation: means, variations and trends during the satellite era (1979–2014). *Surveys in Geophysics*, 38(4), 679-699. http://doi.org/10.1007/s10712-017-9416-4.

Ahmadi, N., Muniruzzaman, M., Sprocati, R., Heck, K., Mosthaf, K., & Rolle, M. (2022). Coupling soil/atmosphere interactions and geochemical processes: a multiphase and multicomponent reactive transport approach. *Advances in Water Resources*, 169, 104303. http://doi.org/10.1016/j.advwatres.2022.104303.

Albrecht, R.I., Goodman, S.J., Buechler, D.E., Blakeslee, R.J., & Christian, H.J. (2016). Where are the lightning hotspots on Earth? *Bulletin of the American Meteorological Society*, 97(11), 2051-2068. http://doi.org/10.1175/BAMS-D-14-00193.1.

Almagro, A., Oliveira, P.T.S., Nearing, M.A., & Hagemann, S. (2017). Projected climate change impacts in rainfall erosivity over Brazil. *Scientific Reports*, 7(1), 8130. http://doi.org/10.1038/s41598-017-08298-y.

Almeida, A.J.G.A., Lira, B.S., Gomes, G.J.C., Jucá, J.F.T., Mariano, M.O.H., & Motta Sobrinho, M.A. (2024). Geotechnical study of oxidative covering layers for sanitary landfills. *Revista de Gestão Social e Ambiental*, 18(10), e08927. http://doi.org/10.24857/rgsa.v18n10-199.

Amaral, C., Silva, A., Lima, I., Ramalho, J., Varejão, S., Rodrigues, J.G., Lago, L., Correia, R., Correa, S., Portocarrero, H., Motta, M., Vargas Junior, E., de Campos, T.M.P., Dourado, F., Silva, L.M., Araújo, J.P.C., Fernandes, N.F., & Vieira, B. (August, 2013). The catastrophic landslide event of january 2011 in Rio de Janeiro: geomorphological and geological controls. In *8th International Conference on Geomorphology*, Paris. Paris: IAG.

An, N., Hemmati, N.A.S., & Cui, Y. (2017). Numerical analysis of soil volumetric water content and temperature variations in an embankment due to soil-atmosphere interaction. *Computers and Geotechnics*, 83, 40-51. http://doi.org/10.1016/j.compgeo.2016.10.010.

Anderson, M.G., Hubbard, M.G., & Kneale, P.E. (1982). The influence of shrinkage cracks on pore-water pressures within a clay embankment. *Quarterly Journal of Engineering Geology*, 15(1), 9-14. http://doi.org/10.1144/GSL.QJEG.1982.015.01.03.

Andrade, J.A. (2019). Balanço hídrico do solo pelo método de Thornthwaite-Mather e classificação racional dos climas pelo método de Thornthwaite [Class notes]. Repository Évora University. Retrieved in January 31, 2025, from http://dspace.uevora.pt/rdpc/bitstream/10174/26075/1/Balan%c3%a7o%20H%c3%addrico%20do%20solo.pdf

Araujo, R., & de Campos, T.M.P. (2013). Uso dos ensaios de penetração de cone, desagregação, sucção e resistência à tração para avaliar erodibilidade. *Geotecnia*, 128(128), 67-85. http://doi.org/10.14195/2184-8394_128_4.

Araujo, R.M.N., Melo, N.R., Cavalcanti, C.P.S., Silva, Á.J.S., Silva, A.G.A., & Bezerra, G.G. (2018). Análise da ocorrência de erosão hídrica no bairro Arlindo Cavalcante, município de Bonito-PE. In *XIX Congresso Brasileiro de Mecânica dos Solos e Engenharia Geotécnica,* Salvador. São Paulo: ABMS.

Associação Brasileira de Resíduos e Meio Ambiente – ABREMA. (2023). *Panorama dos resíduos sólidos no Brasil 2023* (54 p.). São Paulo: ABREMA.

Avelar, A.S., Coelho Netto, A.L., Lacerda, W.A., Becker, L.B., & Mendonça, M.B. (2011). Mechanisms of the recent catastrophic landslides in the mountainous range of Rio de Janeiro, Brazil. In C. Margottini, P. Canuti, & K. Sassa (Eds.), *Proceedings of the 2nd World Landslide Forum. Landslide Science and Practice* (pp. 265-270). Rome: FAO.

Bass, H.E. (1980). The propagation of thunder through the atmosphere. *The Journal of the Acoustical Society of America*, 67(6), 1959-1966. http://doi.org/10.1121/1.384354.

Belfort, N.T., Santana, D.S., Neves, J.P.S., Brito, A.R., & Jucá, J.F.T. (2018). Suction, water retention capacity and permeability assessment of compacted and unsaturated cover layer. *International Journal of Advanced Engineering Research and Science*, 5(10), 200-207. http://doi.org/10.22161/ijaers.5.10.27.

Beneveli, R.M. (2002). *Estudo dos efeitos de umedecimento e secagem na resistência ao cisalhamento de um solo compactado em laboratório* [Master's dissertation]. Pontifícia Universidade Católica do Rio de Janeiro.

Beneveli, R.M., & De Campos, T.M.P. (2004). Drying effects followed by saturation in the strength of a laboratory compacted soil. In O.M. Vilar (Ed.), *5th Brazilian Symposium on Unsaturated Soils* (Vol. 1, pp. 9-14), São Carlos, SP. São Paulo: Universidade de São Paulo. (in Portuguese).

Bennetts, V.H., Lilienthal, A.J., Neumann, P.P., & Trincavelli, M. (2012). Mobile robots for localizing gas emission sources on landfill sites: is bio-inspiration the way to go? *Frontiers in Neuroengineering*, 4, 20.

Bishop, A.W. (1959). The principle of effective stress. *Teknisk Ukeblad*, 106(39), 859-863.

Bordoni, M., Bittelli, M., Valentino, R., Vivaldi, V., & Meisina, C. (2021). Observations on soil-atmosphere interactions after long-term monitoring at two sample sites subjected to shallow landslides. *Bulletin of Engineering Geology and the Environment*, 80(10), 7467-7491. http://doi.org/10.1007/s10064-021-02334-y.

Borma, L.S., Gitirana Junior, G.F.N., & Luiz, G.C. (2023). Soil-vegetation-atmosphere interaction and the role of unsaturated soils. In Comissão Técnica de Solos Não Saturados (Org.), Unsaturated soils in the geotechnical context (Chapter 14, pp. 439-478). São Paulo: ABMS. (in Portuguese).

Borma, L.S., Nobre, C.A., & Cardoso, M.F. (2013). Response of the Amazon tropical forests to deforestation, climate, and extremes, and the occurrence of drought and fire. R.A. Pielke (Ed.), *Climate vulnerability: understanding and addressing threats to essential resources* (1st ed., pp. 153-163). Amsterdam: Academic Press. http://doi.org/10.1016/B978-0-12-384703-4.00228-8.

Boscov, M.E.G., di Emidio, G., Ferrari, A.A.P., Hemsi, P.S., Machado, M.F.C., Machado, S.L., Maia Nobre, M.M., & Maia Nobre, R.C. (2025). Environmental geotechnics: Brazilian experience and some hot topics. *Soils & Rocks*, *48*(3). (in Press).

Brand, E.W. (1985). Predicting the performance of residual soil slopes. In *11th International Conference on Soil Mechanics and Foundation Engineering* (Vol. 5, pp. 2541-2578), San Francisco. Rotterdam: A.A. Balkema Publishers.

Brasil. Ministério da Ciência, Tecnologia e Inovações – MCTI. (2021). *Fourth Brazilian communication to the United Nations convention on climatic changes* (620 p.). Brasília: Ministério da Ciência, Tecnologia e Inovações. (in Portuguese).

Busch, A., & Amorim, S. (2011). The tragedy of the highlands Serrana region in the State of Rio de Janeiro in 2011: looking for answers. *ENAP: Case Study Libray on Public Management*. Retrieved in January 31, 2025, from https://repositorio.enap.gov.br/jspui/bitstream/1/2197/1/case_study_the%20tragedy_of_the_highlands_serrana_region.pdf

Cai, F., & Ugai, K. (2004). Numerical analysis of rainfall effects on slope stability. *International Journal of Geomechanics*, 4(2), 69-78. http://doi.org/10.1061/(ASCE)1532-3641(2004)4:2(69).

Camapum de Carvalho, J. (2023). Erosão no Cerrado sob diferentes olhares. In H.A.S. Loureiro & A.J.T. Guerra (Eds.), *Erosão em áreas Tropicais* (1. ed., pp. 75-116). Rio de Janeiro: Editora Interciência. (in Portuguese).

Camapum de Carvalho, J. (2024). Erosão hídrica no Brasil, um país de clima tropical. In M.M. Sales, M.P. Luz, M.M.A. Mascarenha, J.C. Carvalho, & V.D. Silva (Eds.), *Erosão hídrica dos sedimentos em reservatórios* (1. ed., pp. 57-92). Goiânia: Escola de Engenharia Civil e Ambiental. (in Portuguese).

Camapum de Carvalho, J., & Diniz, N.C. (2007). *Cartilha erosão* (3. ed.). Brasília: Universidade de Brasília; Fundação de Empreendimentos Científicos e Tecnológicos – FINATEC. (in Portuguese).

Camapum de Carvalho, J., & Lelis, A.C. (2006). *Cartilha meio ambiente: erosão* (1. ed.). Brasília: Fundação de Empreendimentos Científicos e Tecnológicos – FINATEC. (in Portuguese).

Camapum de Carvalho, J., Gitirana Junior, G.F.N., Luz, M.P., Sales, M.M., Souza, N.M., & Romão, P.A. (2024). A erosão hídrica e o assoreamento de reservatórios. In M.M. Sales, M.P. Luz, M.M.A. Mascarenha, J.C. Carvalho, & V.D. Silva (Eds.), *Erosão hídrica dos sedimentos em reservatórios* (1. ed., pp. 35-55). Goiânia: Escola de Engenharia Civil e Ambiental. (in Portuguese).

Camapum de Carvalho, J., Lelis, A.C., Sales, M.M., Mascarenha, M.M. dos A., Angelim, R.R., & Luz, M.P. (2016). *Cartilha erosão em borda de reservatório*. Goiânia: Universidade Federal de Goiás. (in Portuguese).

Camapum de Carvalho, J., Lima, M.C., & Mortari, D. (maio, 2001). Considerações sobre prevenção e controle de voçorocas. In *VII Simpósio Nacional de Controle de Erosão*, Goiânia, GO. Goiânia: ABGE. (in Portuguese).

Camapum de Carvalho, J., Pérez, A.C., & Cabral, R.M. (2023). Insumos minerais: diálogo entre o ser humano, o solo, a água, o ar, os elementos químicos e o bioma cerrado. In J. Camapum de Carvalho (Ed.), *Diálogos geotécnicos: convite à reflexão* (2. ed., pp. 251-280). Brasília: José Camapum de Carvalho. (in Portuguese).

Camapum de Carvalho, J., Sales, M.M., Mortari, D., Fázio, J.A., & Motta, N.O., & Francisco, R.A. (2006). In J. Camapum De Carvalho, M.M. Sales, N.M. Souza, & M.T.S. Melo (Eds.), *Processos erosivos no Centro-Oeste Brasileiro*. Brasília: Universidade de Brasília; FINATEC. (in Portuguese).

Carnavale, T.S. (2013). *Desenvolvimento de um modelo físico para análise dos efeitos de réplicas de trovões em solos* [Master's dissertation]. Pontifícia Universidade Católica do Rio de Janeiro.

Carnavale, T.S. (2018). *Soil-Thunder interaction: a field monitoring analysis* [Doctoral thesis]. Pontifícia Universidade Católica do Rio de Janeiro.

Carnavale, T.S., De Campos, T.M.P., & Oliveira, A.R.M.B. (2014). Response of tensiometers to laboratory thunder sound replicated waves. In A.R. Russell (Ed.), *Unsaturated soils: research and applications*. London: CRC Press. http://doi.org/10.1201/b17034-251.

Carnavale, T.S., Motta, M.F.B., de Campos, T.M.P., Alves, H.D.L., Oliveira, A.R.M.B., & Martins, H.J.A. (2016). Unconfined strength of an unsaturated residual soil struck by replicated lightning. In *3rd European Conference on Unsaturated Soils - E-UNSAT 2016* (Vol. 9, pp. 14006), Paris. Les Ulis: EDP Sciences.

Carvalho, C.O.C., de Campos, T.M.P., & Viana, A.F. (2025). Internal erosion processes in homogeneous earth fill dams: a case study. *Soils and Rocks*, 48(1), 22025010923. http://doi.org/10.28927/SR.2025.010923.

Chai, H., Rao, S., Wang, R., Liu, J., Huang, Q., & Mou, X. (2015). The effect of the geomorphologic type as surrogate to the time factor on digital soil mapping. *Open Journal of Soil Science*, 5(6), 123-134. http://doi.org/10.4236/ojss.2015.56012.

Chen, Y., Lai, Y., Zhang, M., Li, H., & Zhang, Y. (2024). A new framework for assessing the evolution of unsaturated soil slope stability under the impact of land-atmosphere interaction: formulation and application. *Computers* *and Geotechnics*, 173, 106542. http://doi.org/10.1016/j.compgeo.2024.106542.

Chen, Y., Li, Q., Wu, W., Liu, X., Cheng, J., Deng, X., Cai, X., Yuan, W., Xie, J., Zhang, S., & Wang, B. (2022). Effects of lightning on rhizosphere soil properties, bacterial communities, and active components of *Camellia sinensis* var. *assamica*. *Frontiers in Microbiology*, 13, 911226. http://doi.org/10.3389/fmicb.2022.911226.

Ching, R.K.H., Sweeney, D.J., & Fredlund, D.G. (1984). Increase in factor of safety due to soil suction for two Hong Kong slopes. In *Fourth International Symposium on Landslides* (pp. 617-623), Toronto. Vancouver: Canadian Geotechnical Society.

Ciência é Tudo. (2022). *Why Brazil is the lightning incidence world champion*. Brasília: TV Brasil. (in Portuguese). Retrieved in January 31, 2025, from https://tvbrasil.ebc.com.br/ciencia-e-tudo/2022/02/descubra-por-que-o-brasil-e-campeao-mundial-na-incidencia-de-raios

Clarkson, L., & Williams, D. (2021). An overview of conventional tailings dam geotechnical failure mechanisms. *Mining, Metallurgy & Exploration*, 38(3), 1305-1328. http://doi.org/10.1007/s42461-021-00381-3.

Coelho Netto, A.L., Sato, A.M., Avelar, A.S., Vianna, L.G.G., Araújo, I.S., Ferreira, D.L.C., Lima, P.H., Silva, A.P.A., & Silva, R.P. (2011). The extreme landslide disaster in Brazil. In C. Margottini, P. Canuti, & K. Sassa (Eds.), *Proceedings of the Second World Landslide Forum* (Vol. 6, pp. 377-384), Rome, Italy. Berlin: Spinger-Verlag.

Collins, B.D., & Stock, G.M. (2016). Rockfall triggering by cyclic thermal stressing of exfoliation fractures. *Nature Geoscience*, 9(5), 395-400. http://doi.org/10.1038/ngeo2686.

Conceição, M.P., Pinto, C.M.T., Lima, F.A.V., & Machado, S.L. (2021). Influence of soil-atmosphere interactions and unsaturated soil properties on slope stability. *MATEC Web of Conferences*, 337, 03019. http://doi.org/10.1051/matecconf/202133703019.

Conciani, W., Burgos, P.C., & Bezerra, R.L. (2023). Origin and soil formation, weathering profiles. In Comissão Técnica de Solos Não Saturados (Ed.), *Unsaturated soils in the geotechnical context* (Chap. 3, pp. 69-90). São Paulo: ABMS. (in Portuguese).

Coutinho, R.Q., Ehrlich, M., Futai, M.M, Bressani, L.A., & de Morais, B.D. (2025). Gravitational mass movements in Brazil: causes, consequences, and solutions. *Soils & Rocks*, *48*(3). (in Press).

Crozier, M.J. (2010). Deciphering the effect of climate change on landslide activity: a review. *Geomorphology*, 124(3-4), 260-267, 260-267. http://doi.org/10.1016/j.geomorph.2010.04.009.

Cui, Y. (2022). Soil-atmosphere interaction in earth structures. *Journal of Rock Mechanics and Geotechnical Engineering*, 14(1), 35-49. http://doi.org/10.1016/j.jrmge.2021.11.004.

Cui, Y.J., Ta, A.N., Hemmati, S., Tang, A.M., & Gatmiri, B. (2013). Experimental and numerical investigation of soil-atmosphere interaction. *Engineering Geology*, 165, 20-28. http://doi.org/10.1016/j.enggeo.2012.03.018.

Cui, Y.J., Tang, C.S., Tang, A.M., & Ta, A.N. (2014). Investigation of soil desiccation cracking using an environmental chamber. *Rivista Italiana di Geotecnica*, *48*(1), 9-20.

Cunha, A.P.M.A., Zeri, M., Leal, K.D., Costa, L., Cuartas, L.A., Marengo, J.A., Tomasella, J., Vieira, R.M., Barbosa, A.A., Cunningham, C., Garcia, J.V.C., Broedel, E., Alvalá, R., & Ribeiro-Neto, G. (2019). Extreme drought events over Brazil from 2011 to 2019. *Atmosphere*, 10(11), 642. http://doi.org/10.3390/atmos10110642.

Damasceno, L.A.G., Carvalho, M.F., & Machado, S.L. (2019). Fugitive methane emissions through the cover system of a Brazilian landfill cell. *Journal of Environmental Engineering and Science*, 14(3), 168-178. http://doi.org/10.1680/jenes.19.00005.

de Campos, T.M.P. (1997). Resistência ao cisalhamento de solos não saturados. In *3° Simpósio Brasileiro de Solos Não Saturados* (Vol. 2, pp. 399-417). São Paulo: ABMS.

de Campos, T.M.P., & Carrillo, C.W. (1995). Direct shear testing on unsaturated soil from Rio de Janeiro. *Proceedings Unsaturated Soils*, *1*, 31-38.

de Campos, T.M.P., Motta, M.F.B., Carnavale, T.S., Vargas Junior, E.A., & Oliveira, A.R.M.B. (2018). Failure mechanisms of unsaturated soil slopes under rainstorms in Rio de Janeiro, Brazil: an overview. *ASCE GSP*, 300, 69-92. http://doi.org/10.1061/9780784481677.004.

de Campos, T.M.P., Carvalho, T.M.O., & Viana, A.C.C. (2021a). Total volume change measurement of unsaturated soil in triaxial tests: a new approach. *Geotechnical Testing Journal*, 44(2), 392-406. http://doi.org/10.1520/GTJ20200002.

de Campos, T.M.P., Viana, A.C.C., Silva, T.A., & Abrantes, L.G. (2021b). Evaluation of the at-rest coefficient of earth pressure in unsaturated residual soil with a new suction-controlled device. *Geotechnical Testing Journal*, 44(2), 373-391. http://doi.org/10.1520/GTJ20190438.

Dehn, M., Burger, G., Buma, J., & Gasparetto, P. (2000). Impact of climate change on slope stability using expanded downscaling. *Engineering Geology*, 55(3), 193-204. http://doi.org/10.1016/S0013-7952(99)00123-4.

Di Donna, A., & Laloui, L. (2015). Response of soil subjected to thermal cyclic loading: experimental and constitutive study. *Engineering Geology*, 190, 65-76. http://doi.org/10.1016/j.enggeo.2015.03.003.

Dijkstra, T.A., & Dixon, N. (2010). Climate change and slope stability in the UK: challenges and approaches. *Quarterly Journal of Engineering Geology and Hydrogeology*, 43(4), 371-385. http://doi.org/10.1144/1470-9236/09-036.

Dunn, R.J.H., Herold, N., Alexander, L.V., Donat, M.G., Allan, R., Bador, M., Brunet, M., Cheng, V., Ibadullah, W.M.W., Ibrahim, M.K.I.B., Kruger, A., Kubota, H., Lippmann, T.J.R., Marengo, J., Mbatha, S., McGree, S., Ngwenya, S., Pabon Caicedo, J.D., Ramos, A., Salinger, J., van der Schrier, G., Srivastava, A., Trewin, B., Yáñez, R.V., Vazquez-Aguirre, J., Jiménez, C.V., Vose, R., Yussof, M.N.A.B.H., & Zhang, X. (2024). Observed global changes in sector-relevant climate extremes indices: an extension to HadEX3. *Earth and Space Science (Hoboken, N.J.)*, 11(4), e2023EA003279. http://doi.org/10.1029/2023EA003279.

Elia, G., Cotecchia, F., Pedone, G., Vaunat, J., Vardon, P.J., Pereira, C., Springman, S.M., Rouainial, M., Esch, J.V., Koda, E., Josifovski, J., Nocilla, A., Askarinejad, A., Stirling, R., Helm, P., Lollino, P., & Osisnski, P. (2017). Numerical modelling of slope–vegetation–atmosphere interaction: an overview. *Quarterly Journal of Engineering Geology and Hydrogeology*, 50(3), 249-270. http://doi.org/10.1144/qjegh2016-079.

Elmi, C., Chen, J., David Goldsby, D., & Gieré, R. (2017). Mineralogical and compositional features of rock fulgurites: A record of lightning effects on granite. *The American Mineralogist*, 102(7), 1470-1481. http://doi.org/10.2138/am-2017-5971.

Entralgo, J.F.T. (2013). *Análise espacial e estatística dos movimentos de massa deflagrados pelas chuvas dos dias 11 e 12 de janeiro de 2011 na região serrana do estado do Rio de Janeiro, Brasil* [Master’s dissertation]. Universidade de Brasília.

Fernandes, N.F., Amaral, C., Bierman, P., Silva, L.M., Araújo, J.P.C., Vargas Junior, E., De Campos, T.M.P., Dourado, F., Lopes, M., Peixoto, M.N.O., & Nunes, A. (2013). Debris flows in Rio de Janeiro: mapping, modeling and dating. In *8th International Conference on Geomorphology*, Paris. Paris: IAG.

Fernández-Pato, J., Gracia, J.L., & Garcia-Navarro, P. (2018). A fractional order infiltration model to improve the simulation of rainfall/runoff in combination with a 2D shallow water model. *Journal of Hydroinformatics*, 20(4), 898-916. http://doi.org/10.2166/hydro.2018.145.

Fityus, S., Walsh, P., & Kleeman, P. (1998). The influence of climate as expressed by the Thornthwaite Index on the design depth of moisture change of clay soils in the Hunter Valley. In *Conference on Geotechnical Engineering and Engineering Geology in the Hunter Valley* (pp. 251-265), Newcastle, NSW. Brisbane: AGS.

Fredlund, D.G. (1979). Second Canadian geotechnical colloquium: appropriate concepts and technology for unsaturated soils. *Canadian Geotechnical Journal*, 16(1), 121-139. http://doi.org/10.1139/t79-011.

Fredlund, D.G., Houston, S.L., Nguyen, Q., & Fredlund, M.D. (2010). Moisture movement through cracked clay soil profiles. *Geotechnical and Geological Engineering*, 28(6), 865-888. http://doi.org/10.1007/s10706-010-9349-x.

Fredlund, D.G., Rahardjo, H., & Fredlund, M.D. (2012). *Unsaturated soil mechanics in engineering practic*e. Hoboken: John Wiley & Sons. http://doi.org/10.1002/9781118280492.

Gama, A.M.C.F., Costa, V.C.B., Firmo, A.B.L., & Jucá, J.F.T. (2019). Study of GHG emissions from solid waste disposal in the metropolitan Recife region. *Ibero-American Journal of Environmental Sciences*, *10*, 6.

Gao, Q.F., Wu, X.Y., Zeng, L., Yu, H.C., & Shi, X.K. (2025). Reliability analysis of soil slope stability considering spatial variability of desiccation cracks. *Computers and Geotechnics*, 179, 106977. http://doi.org/10.1016/j.compgeo.2024.106977.

Gariano, S.L., & Guzzetti, F. (2016). Landslides in a changing climate. *Earth-Science Reviews*, 162, 227-252. http://doi.org/10.1016/j.earscirev.2016.08.011.

Gerscovich, D.M.S., Vargas Junior, E.A., & De Campos, T.M.P. (2006). On the evaluation of unsaturated flow in a natural slope in Rio de Janeiro, Brazil. *Engineering Geology*, 88(1-2), 23-40. http://doi.org/10.1016/j.enggeo.2006.07.008.

Ghosh, D., Banerjee, A., Puppala, A.J., & Kumar, P. (2024). Exploring the influence of climate change on earthen embankments with expansive soil. *Geosciences*, 14(2), 37. http://doi.org/10.3390/geosciences14020037.

Gitirana, G.F.N. (2005). *Weather-related geo-hazard assessment model for railway embankment stability* [Doctoral thesis]. University of Saskatchewan.

Gitirana, G.F.N., Bandeira, A.P.N., Barboza, D.U., Marinho, F.A.M., Camapum de Carvalho, J., Lima, L.B.F., Vilar, O.M., Machado, S.L., Gehling, W.Y., & Núñez, W.P. (2025). Advances in unsaturated soils mechanics and technology in Brazil. *Soils and Rocks*, 43(4), 535-548. http://doi.org/10.28927/SR.2025.009625.

Gomes, K.M.B. (2019). *Avaliação da influência da distribuição da sucção inicial nas condições de fluxo e estabilidade de encostas não saturadas por meio de análises bi e tridimensionais* [Master’s dissertation]. Pontifícia Universidade Católica do Rio de Janeiro.

Gomes, K.M.B., & de Campos, T.M.P. (2022). Evaluation of the influence of initial suction distribution on the flow and stability conditions of unsaturated slopes through bidimensional analysis. In *XX Brazilian Soil Mechanics and Geotechnical Engineering Conference, COBRANSEG 2020*, Campinas, SP. São Paulo: ABMS.

Green, W.H., & Ampt, G.A. (1911). Studies on soil physics, 1: the flow of air and water through soils. *Journal of Agricultural Science*, 4(1), 1-24. http://doi.org/10.1017/S0021859600001751.

Groisman, P.Y., Knight, R.W., Easterling, D.R., Karl, T.R., Hegerl, G.C., & Razuvaev, V.N. (2005). Trends in intense precipitation in the climate record. *Journal of Climate*, 18(9), 1326-1350. http://doi.org/10.1175/JCLI3339.1.

Guerra, A.J.T. (1998). Processos erosivos nas encostas. In S.B. Cunha & A.J.T. Guerra (Eds.), *Geomorfologia: uma atualização de bases e conceitos*. Rio de Janeiro: Bertrand Brasil.

Haque, U., Silva, P.F., Devoli, G., Pilz, J., Zhao, B., Khaloua, A., Wilopo, W., Andersen, P., Lu, P., Lee, J., Yamamoto, T., Keellings, D., Wu, J.H., & Glass, G.E. (2019). The human cost of global warming: deadly landslides and their triggers (1995–2014). *The Science of the Total*

Environment, 682, 673-684. http://doi.org/10.1016/j.scitotenv.2019.03.415.

Haylock, M.R., Peterson, T.C., Alves, L.M., Ambrizzi, T., Anunciação, Y.M.T., Baez, J., Barros, V.R., Berlato, M.A., Bidegain, M., Coronel, G., Corradi, V., Garcia, V.J., Grimm, A.M., Karoly, D., Marengo, J.A., Marino, M.B., Moncunill, D.F., Nechet, D., Quintana, J., Rebello, E., Rusticucci, M., Santos, J.L., Trebejo, I., & Vincent, L.A. (2006). Trends in total and extreme South American rainfall in 1960–2000 and links with sea surface. *Journal of Climate*, 19(8), 1490-1512. http://doi.org/10.1175/JCLI3695.1.

Heckman, K.A., Possinger, A.R., Badgley, B.D., Bowman, M.M., Gallo, A.C., Hatten, J.A., Nave, L.E., SanClements, M.D., Swanston, C.W., Weiglein, T.L., Wieder, W.R., Brian, D., & Strahm, B.D. (2023). Moisture-driven divergence in mineral-associated soil carbon persistence. *Proceedings of the National Academy of Sciences of the United States of America*, 120(7), e2210044120. http://doi.org/10.1073/pnas.2210044120.

Hedan, S., Cosenza, P., Valle, V., Dudoignon, P., Fauchille, A.L., & Cabrera, J. (2012). Investigation of the damage induced by desiccation and heating of Tournemire argillite using digital image correlation. *International Journal of Rock Mechanics and Mining Sciences*, 51, 64-75. http://doi.org/10.1016/j.ijrmms.2012.01.001.

Henn, K.A., & Peduzzi, A. (2024). Surface heat monitoring with high-resolution UAV. *Remote Sensing*, 16(5), 930. http://doi.org/10.3390/rs16050930.

Hillel, D. (1998). *Environmental soil physics: fundamentals, applications, and environmental considerations* (771 p.). New York: Academic Press.

Hobeichi, S., Abramowitz, G., Evans, J.P., & Ukkola, A. (2022a). Toward a robust, impacted-based, predictive drought metric. *Water Resources Research*, 58(2), e2021WR031829. http://doi.org/10.1029/2021WR031829.

Hobeichi, S., Abramowitz, G., Ukkola, A.M., Kauwe, M.D., Pitman, A., Evans, J.P., & Beck, H. (2022b). Reconciling historical changes in the hydrological cycle over land. *NPJ Climate and Atmospheric Science*, 5(1), 17. http://doi.org/10.1038/s41612-022-00240-y.

Honke, R., & Karch, C. (2022). Shock waves from a lightning discharge. In *International Conference on Lightning & Static Electricity*, Madrid. Madrid: ICOLSE.

IMKO. (2009). *Trime-Pico 64/32 user manual*. Marcq-en-Barœul: IMKO. Retrieved in January 31, 2025, from https://envcoglobal.com/trime-pico64-32-manualenglweb0

Intergovernmental Panel on Climate Change – IPCC. (2021). *Climate Change 2021: The Physical Science Basis. Contribution of Working Group I to the Sixth Assessment Report of the Intergovernmental Panel on Climate Change* (2391 p.). Cambridge: Cambridge University Press. Retrieved in January 31, 2025, from https://www.ipcc.ch/re-port/sixth-assessment-report-working-group-i/

Intergovernmental Panel on Climate Change – IPCC. (2023). Contribution of Working Groups I, II and III to the Sixth Assessment Report of the Intergovernmental Panel on Climate Change. In Core Writing Team, H. Lee, & J. Romero (Eds.), *Climate Change 2023: Synthesis Report* (pp. 35-115). Geneva: IPCC.

International Energy Agency – IEA. (2023). *CO2 Emissions in 2022: International Energy Agency Report*. Paris: International Energy Agency.

Iverson, R.M. (2000). Landslide triggering by rain infiltration. *Water Resources Research*, 36(7), 1897-1910. http://doi.org/10.1029/2000WR900090.

Jesus, A.S., Oliveira, M.C., Lima, C.V., Carvajal, H.E.M., Monsalve, G., Londoño, R.D., & Camapum de Carvalho, J. (2023). Influência de aspectos geológicos, hidrogeológicos, geomorfológicos e da cobertura vegetal no estado de saturação do solo. In Comissão Técnica de Solos Não Saturados (Eds.), *Solos não saturados no contexto geotécnico* (2. ed., pp. 159-192). São Paulo: ABMS. http://doi.org/10.4322/978-65-992098-3-3.cap06.

Joris, P.C., Eekhout, J.P.C., & de Vente, J. (2022). Global impact of climate change on soil erosion and potential for adaptation through soil conservation. *Earth-Science Reviews*, *226*. .

Jucá, J.F.T., Norberto, A.S., Santos Junior, J.I., & Marinho, F.A.M. (2021). Brasília municipal solid waste landfill: a case study on flow and slope stability. *Soils & Rocks*, 44(3), 1-13. http://doi.org/10.28927/SR.2021.067321.

Karim, R., Devkota, B., Rahman, M., & Nguyen, H.B.K. (2024). Thornthwaite moisture index and depth of suction change under current and future climate: an Australian study. *Journal of Rock Mechanics and Geotechnical Engineering*, 16(5), 1761-1775. http://doi.org/10.1016/j.jrmge.2023.09.009.

Khalili, N., Romero, E., & Marinho, F.A.M. (2022). State of the art report. advances in unsaturated soil mechanics: constitutive modelling, experimental investigation, and field instrumentation. In M. Rahman & M. Jaksa (Eds.), *Proceedings of the 20th ICSMGE-State of the Art and Invited Lectures* (pp. 297-348). Sydney: Australian Geomechanics Society.

Kodikara, J.K., & Choi, X. (2006). A simplified analytical model for desiccation cracking of clay layers in laboratory tests. *Proceedings of the Fourth International Conference on Unsaturated Soils* (pp. 2558-2569), Carefree, AZ. Reston: ASCE. http://doi.org/10.1061/40802(189)218.

Kossoff, D., Dubbin, W.E., Alfredsson, M., Edwards, S.J., Macklin, M.G., & Hudson-Edwards, K.A. (2014). Mine tailings dams: Characteristics, failure, environmental impacts and remediation. *Applied Geochemistry*, 51, 229-245. http://doi.org/10.1016/j.apgeochem.2014.09.010.

Kramer, M.G., & Chadwick, O.A. (2018). Climate-driven thresholds in reactive mineral retention of soil carbon at the global scale. *Nature Climate Change*, 8(12), 1104-1109. http://doi.org/10.1038/s41558-018-0341-4.

Langenbach, T., Mano, D., Campos, M.M., Cunha, A.L.M.C., & De Campos, T.M.P. (2017). Pesticide dispersion by spraying under tropical conditions. *Journal of Environmental Science and Health. Part B, Pesticides, Food Contaminants, and Agricultural Wastes*, 52(12), 843-849. http://doi.org/10.1080/03601234.2017.1359040.

Lee, S.W. (2009). *Generating synthetic sound of thunder. Sound simulation final project report, COMP 790-058, Computer Science*. Chapel Hill: University of North Carolina.

Levatti, H.U., Prat, P.C., & Ledesma, A. (2019). Numerical and experimental study of initiation and propagation of desiccation cracks in clayey soils. *Computers and Geotechnics*, 105, 155-167. http://doi.org/10.1016/j.compgeo.2018.09.015.

Li, J.H., Li, L., Chen, R., & Li, D.Q. (2016). Cracking and vertical preferential flow through landfill clay liners. *Engineering Geology*, 206, 33-41. http://doi.org/10.1016/j.enggeo.2016.03.006.

Li, L.J.H., Zhang, L., & Kwong, B.C.P. (2011). Field permeability at shallow depth in a compacted fill. *Proceedings of the Institution of Civil Engineers: Geotechnical Engineering*, *164*(3), 211-221.

Lima, M.C. (2003). *Degradação físico-química e mineralógica de maciços junto às voçorocas* [Doctoral thesis]. Universidade de Brasília.

Lima, M.C., Almeida, J.G.R., Medeiros, G.F., Mortari, D., Romão, P.A., Mascarenha, M.M.A. & Camapum de Carvalho, J. (2017). Sulcos, ravinas e voçorocas. In M.M. Sales, J. Camapum de Carvalho, M.M.A. Mascarenha, M.P. Luz, N.M. Souza, & R.R. Angelim (Eds.), *Erosão em Borda de Reservatório* (pp. 65-90). Goiânia: Universidade Federal de Goiás.

Lôbo, B.R.H. (2022). *Uso de canal de fluxo 2D para o monitoramento e avaliação de desempenho de barreiras capilares* [Doctoral thesis]. Universidade Federal da Bahia.

Lôbo, B.R.H., Machado, S.L., & Marques Filho, W.P. (2023). Assessment of cover layers using an instrumented 2D channel with control for climate conditions. *International Journal of Civil Engineering*, 21(9), 1433-1445. http://doi.org/10.1007/s40999-023-00839-z.

Loureiro, H.A.S., & Guerra, A.J.T. (2023). *Erosão em áreas tropicais* (1. ed.). Rio de Janeiro: Interciência.

Lu, N., & Likos, W.J. (2004). *Unsaturated soil mechanics*. Hoboken: John Wiley & Sons, Inc.

Luiz, G.C., Gitirana Junior, G.F.N., Romão, P.A., & Almeida, F.P. (2017). Interação solo-atmosfera e a sua relação com erosão em borda de reservatórios. In M.M. Sales, J. Camapum de Carvalho, M.M.A. Mascarenha, M.P. Luz, N.M. Souza, & R.R. Angelim (Eds.), *Erosão em Borda de Reservatório* (pp. 127-151). Goiânia: Universidade Federal de Goiás.

Luiz, G.C., Martins, L.F.R., & Camapum de Carvalho, J. (2012). A influência do clima na infiltrabilidade do solo. In J. Camapum de Carvalho, G.F.N. Gitirana Junior, & E.T.L. Carvalho (Eds.), *Tópicos sobre infiltração: teoria e prática aplicadas a solos tropicais* (Série Geotecnia UnB, Vol. 4, pp. 49-73). Brasília: Faculdade de Tecnologia.

Lumb, P. (1975). Slope failures in Hong Kong. *Quarterly Journal of Engineering Geology*, 8(1), 31-65. http://doi.org/10.1144/GSL.QJEG.1975.008.01.02.

Maciel, F.J., & Jucá, J.F.T. (2011). Evaluation of landfill gas production and emissions in a MSW large-scale Experimental Cell in Brazil. *Waste Management (New York, N.Y.)*, 31(5), 966-977. http://doi.org/10.1016/j.wasman.2011.01.030.

Mahaney, W.C., & Milner, M.W. (2011). Lightning-induced mineral/chemical changes in red pine (Pinus resinosa). *Palaeogeography, Palaeoclimatology, Palaeoecology*, 309(3-4), 367-373. http://doi.org/10.1016/j.palaeo.2011.07.006.

Maknoon, M., & Aubertin, M. (2021). On the use of bench construction to improve the stability of unsaturated waste rock piles. *Geotechnical and Geological Engineering*, 39(2), 1425-1449. http://doi.org/10.1007/s10706-020-01567-0.

Mandal, D., & Roy, T. (2024). Climate change impact on soil erosion and land degradation. In H. Pathak, D. Chatterjee, S. Saha, & B. Das (Eds.), *Climate change impacts on soil-plant-atmosphere continuum* (Advances in Global Change Research, No. 78). Singapore: Springer. http://doi.org/10.1007/978-981-99-7935-6_5.

Marengo, J.A., Camarinha, P.I., Alves, L.M., Diniz, F., & Betts, R.A. (2021). Extreme rainfall and hydro-geo-meteorological disaster risk in 1.5, 2.0, and 4.0°C global warming scenarios: an analysis for Brazil. *Frontiers in Climate*, V3, 610433. http://doi.org/10.3389/fclim.2021.610433.

Mariano, M.O.H., & Jucá, J.F.T. (2010). Field tests to determine biogas emissions in covering layers of solid waste landfills. *Sanitary and Environmental Engineering*, *15*, 223-228.

Marinho, M.S., do Egito Costa, S.C.F., & Almeida, H.C. (2020). Development of web application for geotechnical classification of tropical soils based on MCT methodology. *Revista de Engenharia Civil IMED*, 7(1), 71-87. http://doi.org/10.18256/2358-6508.2020.v7i1.3373.

Melo, D.L., Kendall, A., & DeJong, J.T. (2023). Review of life cycle assessment (LCA) evaluation of geotechnical systems. In E. Rathje, B.M. Montoya, & M.H. Wayne (Eds.), *Geo-Congress 2023* (pp. 583-592). Reston: ASCE Press. http://doi.org/10.1061/9780784484661.061.

Medeiros, V.S., & De Barros, M.T.L. (2011). Analysis of the critical precipitation events occurred in the mountainous region of the Rio de Janeiro state in the days 11 and 12 of January of 2011. In *XIX Brazilian Symposium on Hydric Resources*, Maceio, AL. Porto Alegre: ABRHidro. (in Portuguese).

Miller, G.A., Hassanikhah, A., & Varsei, M. (2016). Desiccation crack depth and tensile strength in compacted soil. In Z. Chen, C. Wei, D. Sun, & X. Xu (Eds.), *Unsaturated soil mechanics: from theory to practice* (pp. 79–87). London: CRC Press.

Min, S.K., Zhang, X., Zwiers, F.W., & Hegerl, G.C. (2011). Human contribution to more-intense precipitation extremes. *Nature*, 470(7334), 378-381. http://doi.org/10.1038/nature09763.

Mitchell, A.R., & Van Genuchten, M.T. (1993). Flood irrigation of a cracked soil. *Soil Science Society of America Journal*, 57(2), 490-497. http://doi.org/10.2136/sssaj1993.03615995005700020032x.

Mitchell, J.K., Soga, K., & O'Sullivan, C. (2025). *Fundamentals of soil behavior* (4th ed.). Hoboken: John Wiley & Sons.

Momoli, R.S., Camapum de Carvalho, J., & Cooper, M. (2017). Erosão hídrica em solos cultivados. In M.M. Sales, J. Camapum de Carvalho, M.M.A. Mascarenha, M.P. Luz, N.M. Souza, & R.R. Angelim (Eds.), *Erosão em Borda de Reservatório* (pp. 369-397). Goiânia: Universidade Federal de Goiás.

Moncada, M.P.H., De Campos, T.M.P., & Steger, G. (2011). A flexible wall permeameter for measurement of water coefficient of permeability of unsaturated soils. *Geotechnical Testing Journal*, 34(5), 384-395. http://doi.org/10.1520/GTJ103595.

Motta, M.F.B. (2016). *Caracterização físico-hídrico-estrutural e efeito do aumento da pressão do ar na resistência de solos tropicais não saturados* [Doctoral thesis]. Pontifícia Universidade Católica do Rio de Janeiro.

Nakano, M. (1996). Lightning discharge. In C. Uenosono (Ed.), *Lightning: hazards and safeguards* (pp. 27–44). Tokyo: Koeno Kyoikusha.

Newman, M.M., Stahmann, J.R., Robb, J.D., Lewis, E.A., Martin, S.G., & Zinn, S.V. (1967). Triggered lightning strokes at very close range. *Journal of Geophysical Research*, 72(18), 4761-4764. http://doi.org/10.1029/JZ072i018p04761.

Nogami, J.S., & Villibor, D.F. (1981). A new soil classification for roadways application. In *Anais do Simpósio Brasileiro de Solos Tropicais em Engenharia* (pp. 30-47), Rio de Janeiro. São Paulo: ABMS. (in Portuguese).

Nogami, J.S., & Villibor, D.F. (2003). Recent modifications in the MCT geotechnical classification. In *34º Reunião Anual de Pavimentação*, Campinas, SP. Rio de Janeiro: ABPv. (in Portuguese).

Novak, V., Šimåunek, J., & Van Genuchten, M.T. (2000). Infiltration of water into soil with cracks. *Journal of Irrigation and Drainage Engineering*, 126(1), 41-47. http://doi.org/10.1061/(ASCE)0733-9437(2000)126:1(41).

Olaiz, A.H., Singhar, S.H., Vann, J.D., & Houston S.L. (2017). Comparison and applications of the Thornthwaite Moisture Index using GIS. *ASCE GSP*, *302*, 280-289.

Oliveira, C.M.M. (2013) Avaliação de mecanismos de ruptura associados aos escorregamentos da Prainha e Condominio em Nova Friburgo, Rio de Janeiro [Master's dissertation]. Pontifícia Universidade Católica do Rio de Janeiro.

Oliveira, E.P. (2021). *O impacto das mudanças climáticas nos deslizamentos de terra em regiões de clima tropical e subtropical* [Doctoral thesis]. Universidade Federal do Paraná.

Pérez, A.C., & Camapum de Carvalho, J. (2023). Influencia de la adición de insumos agrícolas em las propriedades y el comportamento de los suelos tropicales no saturados. In Comissão Técnica de Solos Não Saturados (Eds.), *Solos não saturados no contexto geotécnico* (2. ed., pp. 533-558). São Paulo: ABMS. http://doi.org/10.4322/978-65-992098-3-3.cap16.

Pinto Junior, O., & Pinto, I.R.C.A. (2020). Lightning changes in response to global warming in Rio de Janeiro, Brazil. *American Journal of Climate Change*, 9(3), 266-273. http://doi.org/10.4236/ajcc.2020.93017.

Portocarrero, H. (2009). *Avaliação do efeito de técnicas de bioengenharia em parâmetros hidrosedimentológicos utilizando instrumentação automatizada* [Doctoral thesis]. Pontifícia Universidade Católica do Rio de Janeiro.

Portocarrero, H., Andrade, A.G., & De Campos, T.M.P. (2017). Monitoramento automatizado do escoamento superficial em parcela experimental instalada em talude de corte. *Geo UERJ*, (30), 277-304.

Portocarrero, H., De Campos, T.M.P., de Andrade, A.G., & Brizzi, R.R. (2021). Hydro-erosive behavior of sedimentary deposits from the Macacu Formation at the Governador Island, RJ. *Revista Brasileira de Geomorfologia*, *22*(3), .

Primavesi, A.B. (1952). *Erosão*. São Paulo: Edições Melhoramentos.

Rahardjo, H., Lee, T.T., Leong, E.C., & Rezaur, R.B. (2005). Response of a residual soil slope to rainfall. *Canadian Geotechnical Journal*, 42(2), 340-351. http://doi.org/10.1139/t04-101.

Rahardjo, H., Ong, T.H., Rezaur, R.B., & Leong, E.C. (2007). Factors controlling instability of homogeneous soil slopes under rainfall. *Journal of Geotechnical and Geoenvironmental Engineering*, 133(12), 1532-1543. http://doi.org/10.1061/(ASCE)1090-0241(2007)133:12(1532).

Rahardjo, H., Satyanaga, A., Leong, E.C., & Song, N.Y. (2010). Effects of groundwater table position and soil properties on stability of slope during rainfall. *Journal of Geotechnical and Geoenvironmental Engineering*, 136(11), 1555-1564. http://doi.org/10.1061/(ASCE)GT.1943-5606.0000385.

Rahimi, A., Rahardjo, H., & Leong, E.C. (2011). Effect of antecedent rainfall patterns on rainfall-induced slope failure. *Journal of Geotechnical and Geoenvironmental Engineering*, 137(5), 483-491. http://doi.org/10.1061/(ASCE)GT.1943-5606.0000451.

Rakov, V.A. (1999). Lightning makes glass. *Journal of the Glass Art Society*, 45-50.

Rakov, V.A., & Uman, M.A. (2003). *Lightning: physics and effects* (3rd ed., Vol. II). Cambridge: Cambridge University Press. http://doi.org/10.1017/CBO9781107340886.

Ramidan, M.A.S. (2003). *Estudo de processo de vossorocamento em área de empréstimo da barragem de Itumbiara, GO*

[Master's dissertation]. Pontifícia Universidade Católica do Rio de Janeiro.

Ramidan, M.A.S., De Campos, T.M.P., Pires Filho, C.J., & Coelho, A.T. (2013). Control of gulling processes near the Itumbiara UHE–GO. *XXIX National Large Dams Seminar*, Porto de Galinhas, PE. Rio de Janeiro: CBDB. (in Portuguese).

Rao, P.P., Ouyang, P.H., Nimbalkar, S., Chen, Q.S., Wu, Z.L., & Cui, J.F. (2022). Analytical modelling of the mechanical damage of soil induced by lightning strikes capturing electro-thermal, thermo-osmotic, and electro-osmotic effects. *Journal of Mountain Science*, 19(7), 2027-2043. http://doi.org/10.1007/s11629-021-7235-z.

Rianna, G., Comegna, L., Mercogliano, P., & Picarelli, L. (2016). Potential effects of climate changes on soil–atmosphere interaction and landslide hazard. *Natural Hazards*, 84(2), 1487-1499. http://doi.org/10.1007/s11069-016-2481-z.

Ribeiro, P.A., Cruz, J.S., Camapum de Carvalho, J., Sales, M.M., Mascarenha, M.M. dos A., da Luz, M.P., & Angelim, R.R. (2016). *Cartilha - Meio Ambiente: Erosão em Borda de Reservatório.* Goiânia: Universidade Federal de Goiás; GECON.

Ribner, S.H., & Roy, D. (1984). *Acoustics of thunder: a quasilinear model for tortuous lightning*. Toronto: University of Toronto.

Richards, L.A. (1931). Capillary conduction of liquids through porous mediums. *Physics*, 1(5), 318-333. http://doi.org/10.1063/1.1745010.

Rocha Júnior, R.L., Silva, F.D.S., Costa, R.L., Gomes, H.B., Pinto, D.D.C., & Herdies, D.L. (2020). Bivariate assessment of drought return periods and frequency in Brazilian Northeast using joint distribution by copula method. *Geosciences*, 10(4), 135. http://doi.org/10.3390/geosciences10040135.

Rouainia, M., Davies, O., O'brien, T., & Glendinning, S. (2009). Numerical modelling of climate effects on slope stability. In *Proceedings of the Institution of Civil Engineers – Engineering Sustainability* (Vol. 162, pp. 81-89). London: Thomas Telford Ltd. http://doi.org/10.1680/ensu.2009.162.2.81.

Sakaki, T., Limsuwat, A., & Illangasekare, T.H. (2011). An improved air pressure measuring method and demonstrated application to drainage in heterogeneous soils. *Vadose Zone Journal*, 10(2), 706-715. http://doi.org/10.2136/vzj2010.0121.

Sales, M.M., Camapum de Carvalho, J., Mascarenha, M.M.A., da Luz, M.P., de Souza, N.M., & Angelim, R.R. (2017). *Erosão em borda de reservatório*. Goiânia: Gráfica UFG.

Sales, M.M., da Luz, M.P., Mascarenha, M.M. dos A., Camapum de Carvalho, J., & da Silva, V.D. (2024). *Erosão hídrica e dinâmica dos sedimentos em reservatórios*. Goiânia: Escola de Engenharia Civil e Ambiental.

Santos, A.P.P., Pinto Junior, O., Santos, S.R.Q., Lima, F.J.L., Souza, E.B., Morais, A.A.R., Ávila, E.E., & Pedernera, A. (2017). Climatic projections of lightning in Southeastern Brazil using CMIP5 models in RCP's scenarios 4.5 and 8.5. *American Journal of Climate Change*, 6(3), 539-553. http://doi.org/10.4236/ajcc.2017.63027.

São Mateus, M.S.C., Machado, S.L., & Barbosa, M.C. (2012). An attempt to perform water balance in a Brazilian municipal solid waste landfill. *Waste Management (New York, N.Y.)*, 32(3), 471-481. http://doi.org/10.1016/j.wasman.2011.11.009.

Scharff, H. (2021). *The impact of management choices on landfill methane emissions: introduction*. Rotterdam: ISWA.

Schirmer, W.N., Jucá, J.F.T., Schuler, A.R.P., Holanda, S., & Jesus, L.L. (2014). Methane production in anaerobic digestion of organic waste from Recife (Brazil) landfill: evaluation in refuse of different ages. *Brazilian Journal of Chemical Engineering*, 31(2), 373-384. http://doi.org/10.1590/0104-6632.20140312s00002468.

Serridge, M., & Licht, T.R. (1987). *Piezoelectric accelerometers and vibration preamplifiers: theory and application handbook* (160 p.). Nærum, Denmark: Brüel & Kjaer.

Silva Junior, A.C. (2015). *Abordagem rítmica probabilística aplicada em análises de fluxo e estabilidade de taludes* [Doctoral thesis]. Universidade de Brasília.

Simunek, J., Sejna, M., & Van Genuchten, M.T. (2005). *The Hydrus-1D software package for simulating the one-dimensional movement of water, heat, and multiple solutes in variably-saturated media*. Riverside: University of California.

Soukatchoff, V.M., & Barbier, M.G. (2023). The effect of natural thermal cycles on rock outcrops: knowledge and prospect. Rock Mechanics and Rock Engineering, 56(9), 6797-6822. http://doi.org/10.1007/s00603-023-03420-1.

Sousa, R.P., Oliveira, I.B., & Machado, S.L. (2011). The use of hydrophobic and hydrophilic tensiometers in the measurement of water and NAPL suctions and determination of SLRC. *Soils & Rocks*, 34(3), 251-258. http://doi.org/10.28927/SR.343251.

Speranza, G., Ferrari, A., & Lassalle, P.L. (2022). Life cycle environmental assessment of retaining walls in unsaturated soils. Geomechanics for Energy and the Environment, 30, 100241. http://doi.org/10.1016/j.gete.2021.100241.

Stocker, T.F., Qin, D., Plattner, G.K., Tignor, M., Allen, S.K., Boschung, J., Nauels, A., Xia, Y., Bex, V., & Midgley, B.M. (2013). *IPCC, 2013: climate change 2013: the physical science basis. Contribution of working group I to the fifth assessment report of the intergovernmental panel on climate change* (1535 p.). Cambridge: Cambridge University Press.

Stoffel, M., Trappmann, D.G., Coullie, M.I., Ballesteros Cánovas, J.A., & Corona, C. (2024). Rockfall from an increasingly unstable mountain slope driven by climate warming. *Nature Geoscience*, 17(3), 249-254. http://doi.org/10.1038/s41561-024-01390-9.

Tang, A.M., Hughes, P.N., Dijkstra, T.A., Askarinejad, A., Cui, Y.J., Diez, J.J., Firgi, T., Gajewska, B., Gentile, F., Grossi, G., Jommi, C., Kehagia, F., Koda, E., ter

Maat, H.W., Lenart, S., Lourenco, S., Oliveira, M., Osinski, P., Springman, S.M., Stirling, R., Toll, D.G., & Van Beek, V. (2018). Atmosphere–vegetation–soil interactions in a climate change context, impact of changing conditions on engineered transport infrastructure slopes in Europe. *Quarterly Journal of Engineering Geology and Hydrogeology*, 51(2), 156-168. http://doi.org/10.1144/qjegh2017-103.

Tang, C.S., Cui, Y.J., Shi, B., Tang, A.M., & Liu, C. (2011b). Desiccation and cracking behaviour of clay layer from slurry state under wetting-drying cycles. *Geoderma*, 166(1), 111-118. http://doi.org/10.1016/j.geoderma.2011.07.018.

Tang, C.S., Shi, B., Liu, C., Gao, L., & Inyang, H.I. (2011a). Experimental investigation of the desiccation cracking behavior of soil layers during drying. *Journal of Materials in Civil Engineering*, 23(6), 873-878. http://doi.org/10.1061/(ASCE)MT.1943-5533.0000242.

Thornthwaite, C.W. (1948). An approach toward a rational classification of climate. *Geographical Review*, 38(1), 55-94. http://doi.org/10.2307/210739.

Thornthwaite, C.W., & Mather, J.R. (1957). Instructions and tables for computing Potential Evapotranspiration and the Water Balance. *Publications in Climatology*, *10*(3).

Thornthwaite,C.W., & Mather, J.R. (1955). *The water balance* (104 p.). Centerton: Drexel Institute of Technology, Laboratory of Climatology.

Tian, X., Li, T., & Gong, W. (2023). Temperature effect on the stability of 3D reinforced slopes under unsaturated flow conditions. *Computers and Geotechnics*, 164, 105771. http://doi.org/10.1016/j.compgeo.2023.105771.

Toll, D.G., Tsaparas, I., & Rahardjo, H. (2001). The influence of rainfall sequences on negative pore water pressures within slopes. In *XV International Conference Soil Mechanics and Geotechnical Engineering* (pp. 1269-1272), Istanbul. London: ISSMGE.

Trenberth, K.E. (2011). Changes in precipitation with climate change. *Climate Research*, 47(1), 123-138. http://doi.org/10.3354/cr00953.

Trenberth, K.E., Dai, A., Rasmussen, R.M., & Parsons, D.B. (2003). The changing character on precipitation. *Bulletin of the American Meteorological Society*, 84(9), 1205-1218. http://doi.org/10.1175/BAMS-84-9-1205.

Tsiampousi, A., Zdravkovic, L., & Potts, D.M. (2016). Soil-atmosphere interaction in unsaturated cut slopes. *E3S Web of Conferences*, 9, 08004. http://doi.org/10.1051/e3sconf/20160908004.

UMS. (2009). *Solos*. Retrieved in January 31, 2025, from http://www.pdinstrumentos.com.br/pt/paginas/minitensiometro_t5/

United Nations Environment Programme – UNEP. (2024). *Emissions Gap Report 2024: No more hot air ... please! With a massive gap between rhetoric and reality, countries draft new climate commitments*. Nairobi: UNEP.

United States. Environmental Protection Agency – EPA. (2018). *Inventory of U.S. Greenhouse Gas Emissions and Sinks: 1990-2017*. Washington, D.C.: U.S. Environmental Protection Agency. Retrieved in January 31, 2025, from https://www.epa.gov/sites/production/files/2019-04/documents/us-ghg-inventory-2019-main-text.pdf

van Breemen, N., & Buurman, P. (2002). *Soil formation* (2nd ed.). Dordrecht: Springer. http://doi.org/10.1007/0-306-48163-4.

Vanicek, I. (2013). The importance of tensile strength in geotechnical engineering. *Acta Geotechnica Slovenica*, *1*, 5-17.

Vargas Junior, E.A., Velloso, R.Q., Chávez, L.E., Gusmão, L., & Amaral, C.P. (2013). On the effect of thermally induced stresses in failures of some rock slopes in Rio de Janeiro, Brazil. *Rock Mechanics and Rock Engineering*, 46(1), 123-134. http://doi.org/10.1007/s00603-012-0247-9.

Wakasa, S.A., Nishimura, S., Shimizu, H., & Matsukura, Y. (2012). Does lightning destroy rocks?: results from a laboratory lightning experiment using an impulse high-current generator. *Geomorphology*, 161-162, 110-114. http://doi.org/10.1016/j.geomorph.2012.04.005.

Waswa, G.W., Lorentz, S.A., & Le Roux, P.A.L. (2011). Rapid mobilization of pre-event water from Hillslopes, a transient pressure wave mechanism. In *15th SANCIAHS National Hydrology Symposium on Science Sustainable Water Resources Management*, South Africa. Grahamstown: Rhodes University.

Westra, S., Fowler, H.J., Evans, J.P., Alexander, L.V., Berg, P., Johnson, F., Kendon, E.J., Lenderink, G., & Roberts, N.M. (2014). Future changes to the intensity and frequency of short-duration extreme rainfall. *Reviews of Geophysics*, 52(3), 522-555. http://doi.org/10.1002/2014RG000464.

Wilson, G.W. (1990). *Soil evaporative fluxes for geotechnical engineering problems* [Doctoral thesis]. University of Saskatchewan.

Zavattini, J.A., & Boin, M.N. (2013). *Climatologia geográfica: teoria e prática de pesquisa*. Campinas: Alínea.

Zhan, T.L.T., Ng, C.W.W., & Fredlund, D.G. (2006). Instrumentation of an unsaturated expansive soil slope. *Geotechnical Testing Journal*, *30*(2), 1-11.

Zhang, J., Zhu, D., & Zhang, S. (2020). Shallow slope stability evolution during rainwater infiltration considering soil cracking state. *Computers and Geotechnics*, 117, 103285. http://doi.org/10.1016/j.compgeo.2019.103285.

Zhang, C., Fang, S., Wang, Y., Shi, X., Yao, Z., & Zhang, T. (2024). Instability prevention and control of waste dump slopes with different consolidation degrees under the influence of rainfall. *Geohazard Mechanics*, *3*(1), 73-86.